University of Stavanger

Faculty of Science and Technology

MASTER'S THESIS

Study program: **Master in Petroleum Technology** Specialization: **Reservoir Engineering**	Autumn semester, December 2012..... **Open**
Writer: **Jose da Costa Ferreira**	…… (Writer's signature)
Faculty supervisor: **Skule Strand**	
Title of thesis: **Low Salinity Effect After Sea Water Flooding In Sandstone Reservoirs**	
Credits (ECTS): **30**	
Key words: - **Enhanced Oil Recovery** - **Waterflooding** - **Low Sal** - **Sandstone** - **Clays** - **Wettability**	Pages: 72 + enclosure: 20 Stavanger, December /2012 Date/year

Frontpage for master thesis
Faculty of Science and Technology
Decision made by the Dean October 30th 2009

ABSTRACT

Clays are the main wetting minerals and have permanently negative surface charges. The negative charges must be balanced by; active cat ions, polar components or H^+.

pH changes is observed in the effluent by flooding in a sequence of FW-SW-LS-FW. The concentration of ions in the Low Salinity brine are lower than in the formation water and sea water brines, especially Ca^{2+}, Mg^{2+}.

In the proposed chemical mechanism on Low Sal EOR effects in sandstone reservoir, it is the effects of pH, both for the adsorption of acidic and basic organic components onto clay minerals, to create initial low water wetness, and also for the desorption of the polar components when the smart water is introduced.

When injecting Low Salinity fluid with low Ca^{2+} concentration, it will promote desorption of Ca^{2+} from the clay surface which consequently creates a local increase in pH close to the brine-clay interface due to H^+ from the water compensates the negative charges at the clay surface. A fast reaction between OH^- and the absorbed acidic and protonated basic material, it will cause desorption of organic material from the clay surface, and as the results, the water wetness of the rock is improved and increased in oil recovery is observed due to increased positive capillary pressure.

Mostly all sandstone reservoirs in North Sea have already been flooded with Sea Water. ***Is it likely to observe Low Salinity EOR effect after the reservoir have been Sea Water flooded?***

Through the combination of theoretical knowledge, and detailed low salinity experiments carried out in the lab, both pH screening tests and oil recovery tests on reservoir cores ***confirmed*** the possibility to observe Tertiary LS EOR effects in a High Temperature Sandstone Reservoir.

TABLE OF CONTENTS

LIST OF TABLES

LIST OF FIGUERES

ACKNOWLEDGEMENTS

Having an opportunity to study as a Masters Student in Petroleum Engineering at the University of Stavanger was truly magnificent and challenging experience for me. I would like to express my sincere gratitude and great appreciation to my Supervisor ***Professor Skule Strand*** for his time, guidance, encouragement, support and inspiration from the beginning to the completion of this project, developed my understanding of the subject. Without him, the completion of this thesis would have not been possible. I have always felt welcome to his office or even in the lab to talk and consult with him.

Special thanks to ***the Norwegian Programme Assistance Project (NPAP) in Corporation with the Government of Timor Leste Through the Ministry of Petroleum and Mineral Resources*** for the financial support during my study at the University of Stavanger, Norway.

I should also thank my parents, brother and sister, dear friends, for your continuously giving support and encouragement through the years until today. Finally I would like to thank my children who always giving encouragement and mental support with eternal love, even without their Mother. It's been a very hard situation within these period after my wife passed away last year. I almost decided not to continue my study. But thinking back to all of the sacrifices that had been done, then I committed myself to continue and reaffirmed that I should finish my study one day, and today I made it happen.

I would also like to express my sincere gratitude to the folks within the Department of Petroleum Engineering who always welcomed me.

Jose da Costa Ferreira

CHAPTER I
INTRODUCTION

1.1. Introduction

Waterflooding is widely applied in the field to improve recovery from oil reservoirs. Yildiz and Morrow (1996) showed that changes in injection-brine composition can improve oil recovery. Thereby introducing the idea that the composition of the brine could be varied to optimize the waterflood recovery. Tang and Morrow (1997)(Tang and Morrow 1999; Morrow et al. 1998; McGuire et al. 2005) built on his idea by demonstrating the benefit of lowering brine salinity on oil recovery.[15]

Zhang and Morrow, 2006; Zhang at al., 2007b, and also by researchers at BP (Larger at al., 2007; Webb et al., 2005b) have confirmed that enhanced oil recovery can be obtained when performing a tertiary low salinity water flood, with salinity in the range of 1000-2000 ppm in test on sandstone cores. Larger et al. (2007) reported that the average increase in recovery was 14%. The laboratory observations have also been confirmed by single well tests performed in an Alaskan reservoir (Larger et al., 2008b) [5]

In the last decade anincreasing amounts of laboratory experiment results have been published, and various suggestions of the mechanism have been proposed. However there are no mechanism generally accepted as the "true" mechanism.

The fact is that there are many parameters linked to the rock, to the reservoir fluids (oil and brine), and to the injection fluid that are involved. In order to give a good background to understand the proposed mechanism of low salinity waterflooding effect in this theses, we will summarize a list of the accepted experimental condition needed, followed by a short recap of the previously suggested mechanism.

The listed conditions for low salinity effects are mostly related to the systematic experimental work by Tang and Morrow (199a), and some of these are also taken from the work done by BP researchers (larger et al., 2007; Larger et al., 2008a).[5, 9, 10]

- Porous medium
  - Low salinity effects have not been documented in pure carbonates, but Put et al., have observed effects in a sandstone containing dolomite crystal (Put et al., 2008).
  - Clay must be present.
  - Sandstones.
- Oil
  - Must contain polar components (i.e. acids and base number).
  - No LS effect have been observed using mineral oils.
- Formation brine
  - Initial water must be present.
  - Formation water must contain divalent cations, i.e. Ca^{2+}, Mg^{2+}, (Larger et al., 2008a).
  - Efficiency is related to initial water saturation Swi.
- Low salinity injection fluid
  - The salinity is usually between 1000 – 2000 ppm, but effects have been observed up to 5000 ppm.
  - There appears to be sensitive to the ionic composition (Ca^{2+}vs Na^{+},)
- Produced water
  - In some cases, production of fines have been detected, but low salinity effects have also been observed without visible production of fines (Larger et al., 2008a).

- It has not been verified that increase in pH is needed to observe low salinity effects.
- From a non-buffered system, the pH of the effluent water usually increase about 1-3 pH units when injecting the low salinity fluid.

- Permeability decrease
  - There is lack of experimental evidence to say that observed low salinity effects are accompanied by permeability reduction.
  - An increase in pressure over the core is detected in some experiments when switching to the low salinity fluid, which may be related to migration of fines formation of an oil/water emulsion.
  - Waterflood experiments have been performed without any variation in end point relative permeability data between high and low salinity waterflood, under both secondary and tertiary flood conditions (Webb et al., 2008).
- Temperature
  - There appears to be no temperature limitations to where low salinity effects can be observed. Most of the reported studies, howeverhave been performed at temperature below 100^0C.

1.2. Description

This master theses is carried out based on experimental studies in the EOR laboratories at the Petroleum Engineering Department at the University of Stavanger.

In this study, reservoir cores from a sandstone reservoir were used. The cores were used in oil recovery studies, and for pH screening.

During the pH screening experiment, 100% FW saturated cores were flooded successively with FW, SW and LS Brine. effluent samples were collected in the sealed glasses for pH, density measurement and ions concentration of Ca^{2+}, Mg^{2+} and SO_4^- analysis.

In the oil recovery studies the cores were saturated with formation water with an initial water saturation of 20% as described in the experimental work. The core then saturated, flooded and aged with stabilized reservoir crude oil.The produced oil was recorded during successively flooding with FW – SW – LS. The pH of the produced water was observed at the effluent.

1.3. Objectives

The objective of this study is to evaluate the possibilities of LS effect after SW flooding in "High Temperature Sandstone Reservoirs".

1.4. Structure of the theses

This thesis begins by introducing general theory in regard to EOR application and mostly referred to the previously alternatives low salinity water flooding mechanism as well as the new proposed chemical mechanism behind the low salinity effect on oil recovery.

This theses consists of six chapters as outlined below:

- Chapter I. Introduction
- Chapter II. Literature Review
- Chapter III. Experimental Work
- Chapter IV. Results
- Chapter V. Discussions
- Chapter VI. Conclusion
- Appendix
- References
- Nomenclature

CHAPTER II
LITERATURE REVIEW

2.1. Definition of EOR

Oil recovery operations traditionally have been subdivided into three stages; primary, secondary, and tertiary. Historically, these stages described the production from reservoir in a chronological sense.

2.1.1. Primary recovery

Primary recovery results from the use of natural energy present in the reservoir as the main source of energy for the displacement of oil to producing wells. These natural energy sources are solution-gas drive, gas-cap drive, natural water drive, fluid and rock expansion, and gravity drainage. On primary recovery stage, the recovery factor is relatively low, around 5 – 30% on average of the original oil in place (Bviere, 1991).

2.1.2. Secondary recovery

Secondary recovery, the second stage of operations, usually was implemented after primary production declined. Traditionally secondary recovery processes are water flooding, pressure maintenance, and gas injection, although the term secondary recovery is now almost synonymous with water flooding. Secondary recovery results from the augmentation of natural energy through injection of water or gas to displace oil towards producing wells. Gas processes based on other mechanisms, oil swelling, oil viscosity reduction, or favorable phase behavior, are considered EOR process. The recovery factor may reach 35 – 50 % of the original oil in place (Green, 1998).[1, 27]

2.1.3. Tertiary recovery

Tertiary recovery, the third stage of production, was obtained after water flooding (or whatever secondary process was used). Tertiary processes used miscible gases, chemical, and/or thermal energy recovery to displace additional oil after the secondary process become uneconomical. Chemicals applied in an EOR process may be surfactants or alkaline agents in which they are injected in a combination of phase behavior and reduction of interfacial tension (IFT) to displace oil. [1, 27]

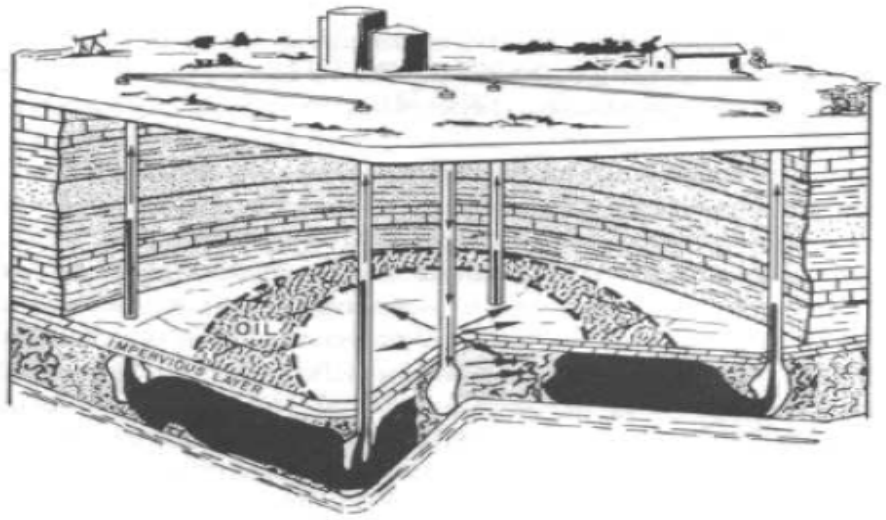

Fig 2.1. Displacement of oil through reservoir rocks by waterflooding (five-spot pattern)(Donaldson et al., 1989)

2.2. Mineralogy and sedimentary rock

Rivers, oceans, winds, and rain runoff all have the ability to carry particles washed off from eroding rock. Such material, called ***detritus***, consist of fragments of rocks and minerals. When the energy of the transporting current is not strong enough to carry these particles, the particles drop out in the process of sedimentation.

This type of sedimentary deposition is referred to as ***clastic sedimentation*** where rocks formed by the accumulation of mostly silicate mineral fragments. These include most sandstones, mud rocks, conglomerates and breccias.

Because of their detrital nature, any mineral can occur in a sedimentary rock. Clay minerals are the dominant material produced by chemical weathering of rocks, and it is mostly abundant in mud rocks. [25, 35, 36]

2.3. Clays

Clay is a general term including many combination of one or more clay types with traces of melt oxides and organic matter. Geological clay deposits are mostly composed of phyllosilicate minerals containing variable amounts of water in the mineral structure.

Clay minerals are typically formed over long periods of time by the gradual chemical weathering of rocks, usually silicate bearing, by low concentrations of carbonic acid and other diluted solvents. These solvents, usually acidic, migrate through the weathering rock after leaching through upper weathering layers. In addition to the weathering process, some clay minerals are formed by hydrothermal activity. Clay deposits may be formed as a result of a secondary sedimentary deposition process after they have been eroded and transported from their original location of formation. Clay deposits are typically associated with very low energy depositional environments such as large lakes and marine basins.

Primary clays, also known as kaolin, are located at the site of formation. Secondary clay deposits have been moved by erosion and water from their primary location.

Clays are distinguished from other fine-grained soils by difference in size and mineralogy. Silts, which are fine-grained soils that do not include clay minerals, tend to have larger particle sizes than clays, but there is some overlap in both particle size and other physical properties, and there are many naturally occurring deposits which include silts and also clay. The distinction

between silt and clay varies by discipline. Geologist and oil scientists usually consider the separation to occur at a particle size of 2µm (clays being finer than silts), sedimentologists often use 4-5µm, and colloid chemists use 1 µm. Geotechnical engineers distinguish between silts and clays based on the plasticity properties of the soil, as measured by the soils. Atteberg Limits. ISO 14688 grades clay particles as being smaller than 2 µm and silts larger.[25, 35, 36, 37]

2.3.1. Properties of Clays

Clay minerals are generally crystalline in nature, and the structure of the clay crystals determines its properties. Typically, clays have a flaky, mica-type structure. Clay flakes are made up of a number of crystal platelets stacked face-to-face. Each platelet is called a unit layer, and the surfaces of the unit layer are called basal surfaces. A unit layer is composed of multiple sheets, where one sheet is called the octahedral sheet. It is consist of either aluminum or magnesium atoms octahedral coordinated with the oxygen atoms of hydroxyl groups. Another sheet is called tetrahedral sheet where consists of silicon atoms tetrahedral coordinated with oxygen atoms. [25, 35, 36, 37]

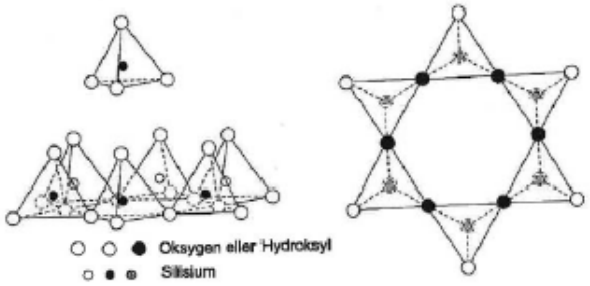

Fig 2.2. Structure of a tetrahedral layer (IDF, 1982)

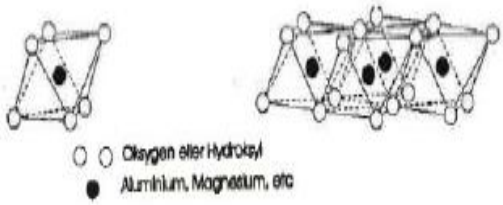

Fig 2.3. Structure of a octrahedral layer (IDF, 1982)

When a linking occurs between one octahedral and tetrahedral sheet, one basal sheet consists of exposed oxygen atoms while the other basal surface has exposed hydroxyl groups.[12]

The unit layers attract together face-to-face and are held in place by weak attractive forces. The distance between corresponding planes in adjacent unit layers is called the c- spacing. A clay structure unit layer consisting of three sheets typically has a c-spacing of about $9.5*10^{-7}$ mm.[12] In clay mineral crystals, atoms having different valences commonly will be positioned within the sheets of the structure to create a negative potential at the crystal surface. In that case, a cation is adsorbed on the surface, and the adsorption cations are called exchangeable cations because they may chemically trade places with other cations when the clay crystal is suspended in the water. In addition, ions may also adsorbed on the crystal edges and exchange with other ions in the water.[12] The type of substitutions occurring within the clay crystal structure and the exchangeable cations adsorbed on the crystal surface greatly affect clay swelling.

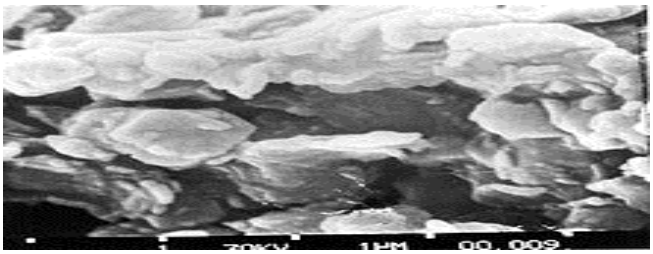

Fig 2.4. Electron microscopic photograph of smectitie clay – magnification 23,500

Depending on the academic source, there are three or four main groups of clays: kaolinite, montmorillite-smectite, illite, and chlorite.

Chlorites are not always considered a clay, sometimes being classified as a separate group within the phyllosilicates. There are approximately 30 different types of pure clays in these categories, but most natural clays are mixtures of these different types, along with other weathered minerals.

2.3.1.1. Kaolinite

Kaolinite is a part of the group of industrial minerals, with has the chemical composition $Al_2Si_2O_5(OH)_4$. It is a layered silicate mineral, which one tetrahedral sheet has the link through oxygen atoms to one octahedral sheet of alumina octahedral. Rocks that more rich in kaolinite are known as kaolin or china clay.

Kaolinite is known as non-swelling clay and the changes within the kaolinite structure are well balance, and therefore a relative low cation exchange capacity as shown in table 2.2. The CEC of kaolinite is mainly linked to the edge surface. The clay has a tendency to transform into illite and chlorite at larger depths (Austad, 2010b).

Kaolinite has low shrink-swell capacity and has a low CEC (cation exchange capacity) (1-15 meq/100g). it is a soft, earthy, usually white mineral (dioctahedralphyllosilicate clay), produced by the chemical weathering of aluminum silicate minerals like feldspar. In many parts of the world, it is pink-orange-red colour by iron oxide. Lighter concentrations is yellow or light orange colour. Alternating layers are sometimes found, as at Providence Canyon State Park in Georgia, USA. Commercial grades of kaolin are supplied and transported as dry powder, semi-dry noodle or as liquid slurry.[25, 35, 36, 37]

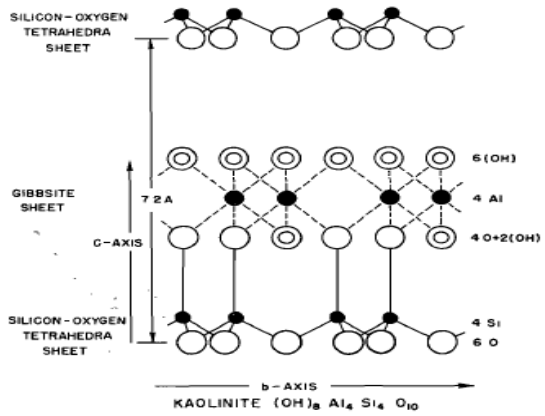

Fig 2.5. Schematic structure Crystal of kaolinite(After Gruner – Grim)(Hughes, 1950)

2.3.1.2. Montmorillonite

Montmorillonite is a very soft clay that typically form in microscopic crystals. Montmorillonite, member of the smectite family. It is a 2:1 clay, meaning that has 2 tetrahedral sheets sandwiching a central octahedral sheet.

Montmorillonite is the main constituent of the volcanic ash weathering product, bentonite. The water content of Montmorillonite is variable and increases greatly in volume when it absorbs water. Chemically it is hydrated sodium calcium aluminum magnesium silicate hydroxide $(Na,Ca)_{0.33}(Al,Mg)_2(Si_4O_{10})(OH)_2{\cdot}nH_2O$. Iron, Potassium, and other cations are common substitutes. Montmorillonite often occurs as intermixed with chlorite, muscovite, illite, cookite, and kaolinite.

Montmorillonite is used in the oil drilling industry as a component of drilling mud. It moderates the mud slurry viscous which helps in cooling the drill bit and removal of drilled solids. Montmorillonite has a very high cation exchange capacity (CEC). it is not suitable for Low Salinity waterflooding because it is a swelling clay,.[25, 35, 36, 37]

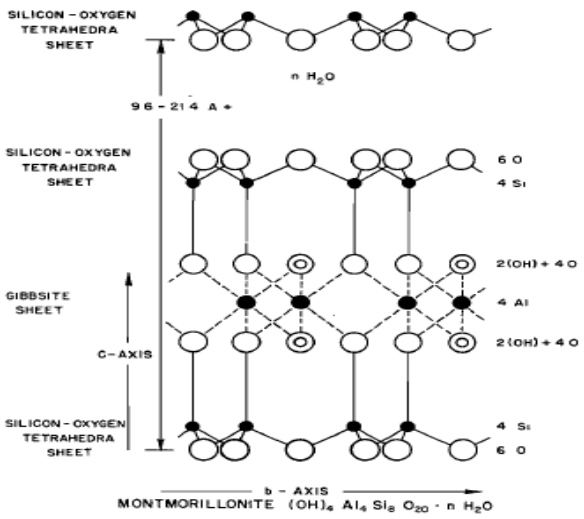

Fig 2.6. Schematic Crystal of structure of montmorillonite (After Hoffman, Endell, and Wilm.-Grim) (Hughes, 1950)

2.3.1.3. Illite

Illite is a non-expanding, clay-sized, micaceus minerals. The structure of illite is constituted by the repetition of tetrahedron – octahedron – tetrahedron (TOT) layers, termed 2:1 structure. The interlayer space is mainly occupied by poorly hydrated potassium cations that responsible for the absence of swelling. Structurally illite is quite similar to muscovite which slightly has more silicon, magnesium, iron, and water and slightly less tetrahedral aluminum and interlayer potassium. It appears as aggregates of small monoclinic grey to white crystal. Due to the small size, it usually requires XRD (x-ray diffraction) or SEM-EDS (automated mineralogy) analysis for best identification. Illite appears as an alteration product of muscovite and feldspar in weathering and hydrothermal environments. [25, 35, 36, 37]

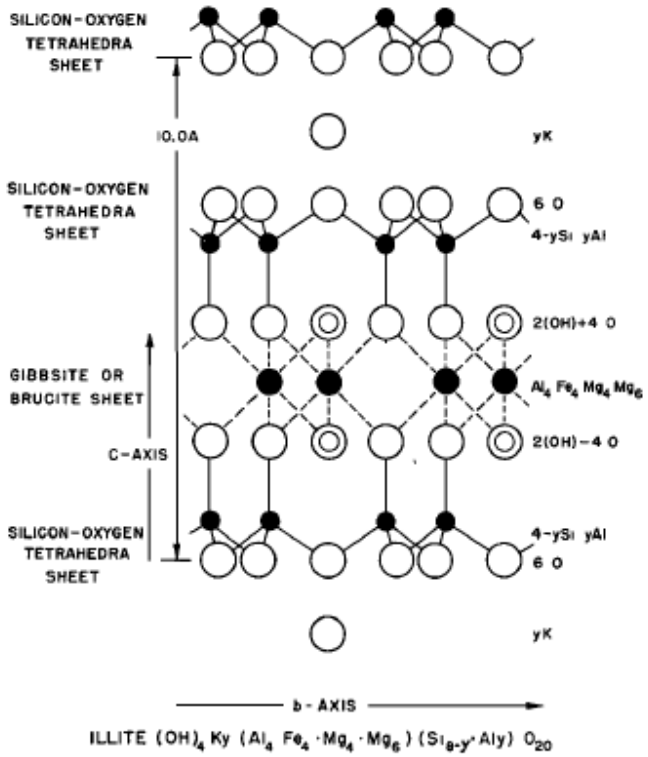

Fig 2.7. Schematic Crystal of structure of Illite(After Grim, Bray, and Bradley) (Hughes, 1950)

2.3.1.4. Chlorite

The chlorites are a group of phyllosilicate minerals. Chlorites can be described by the following four members based on their chemistry composition.

- Clinochlore; $(Mg_5Al)(AlSi_3)O_{10}(OH)_8$
- Chamosite ; $(Fe_5Al)(AlSi_3)O_{10}(OH)_8$
- Nimite; $(Ni_5Al)(AlSi_3)O_{10}(OH)_8$
- Pennantite: $(Mn,Al)_6(Si,Al)_4O_{10}(OH)_8$

The great range in composition results in considerable variation in physical, optical, and x-ray properties. The range of chemical composition allows chlorite group minerals to stand over pressure and wide range of temperature conditions. For this reason chlorite minerals are ubiquitous minerals within low and medium temperature rocks, hydrothermal rocks and deeply buried sediments.

Chlorite has a very large surface area, but the cation exchange capacity is in the same range as for mica/illite. It is the same with kaolinite where the edge surface will be the active place for cation exchange capacity.[25, 35, 36]

Table 2.2. Properties of clay minerals (IDF 1982)

Property	Kaolinite	**Illite/mica**	**Montmorillonite**	**Chlorite**
Layers	1:1	2:1	2:1	2:1:1
Particle size (micron)	5 – 0.2	Large sheets To 0.5	2 – 0.1	5 – 0.1
Cationexchange capacity (100/100g)	3 - 15	10 - 40	80 - 150	10 - 40
Surface area BET – N2 (m^2/g)	15 - 25	50 - 110	30 - 90	140

2.3.2. Swelling of clays

There are two types of swelling may occur, where the surface hydration is one type of swelling in which water molecules are adsorbed on crystal surfaces. Hydrogen bonding holds a layer of water molecules to the oxygen atoms exposed on the crystal surfaces. Subsequent layer of water molecules align to form a quasi-crystalline structure between unit layers which results in an increased c-spacing. All types of clays swell in this manner.[12]

The second swelling is called osmotic swelling. The concentration of cations between unit layers in a clay mineral is higher than the cations concentration in the surrounding water. When the water between the unit layers is osmotically drawn, the c-spacing is increased. Consequently osmotic swelling results increase in overall volume larger than surface hydration. However only certain clays, like sodium montmorullonite, swell in this manner.

Exchangeable cations found in clay minerals were reported to have a significant impact on the amount of swelling that takes place. The exchangeable cations compete with water molecules for the variable reactive sites in the clay structure. In general cations which high valences are more strongly adsorbed rather than with low valence. Thus, the exchangeable cations of clays with low valence will swell more than clays that have exchangeable cations have higher valence.[12, 25, 35, 36, 37]

2.4. Wettability

Wettability is " *the tendency of one fluid to spread or adhere to a solid surface in the presence of other immiscible fluid*" (Graig 1971). Wettability describes the relative preference of a rock to be covered by a certain phase. Rock is defined to be water-wet if the rock has much more affinity for water than for oil. In that case, a major part of the rock surface in the pores will be covered with a water layer. It is clearly that wettability will be effected by the minerals present in the pores. In Sandstones reservoir rock is usually found to be mixed-wet.

Basic reservoir properties such as relative permeability, capillary pressure and resistivity depend strongly on wettability. It is therefore important that laboratory experiments in which these properties are measured are carried out on samples whose wettability is representative of the reservoir from which they are taken.[8, 16, 20]

The wettability of the reservoir rock plays important role in the determination of residual oil saturation and recovery efficiency during the water flooding process. Rock wettability can be indicated by using contact angle technique where for oil/water system, if the contact angle is (0-75^0) the rock is water wet, (75-115^0) intermediate, and (115-180^0) is oil-wet (Anderson 1986).

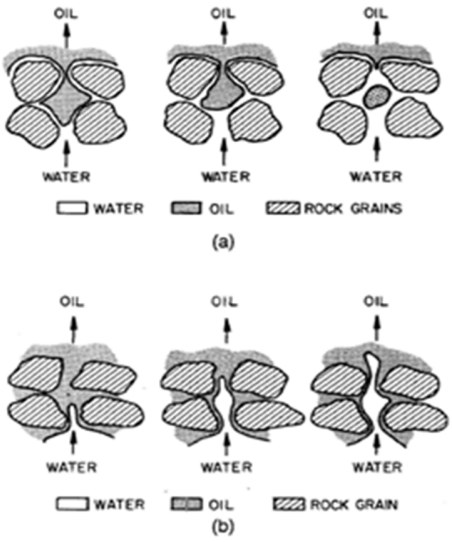

Fig 2.8. (a) Water displacing oil form a pore during awaterflooding (Strongly water-wet rock) and (b) strongly oil-wet rock (Reza et al.)

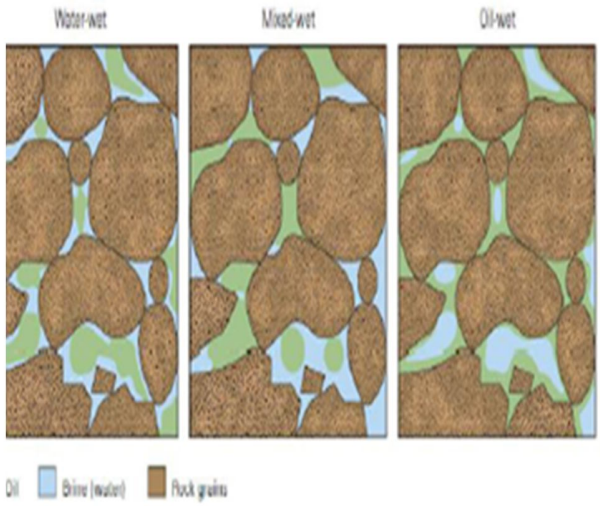

(c)

(c)Pore Scale Distribution of Fluids in the Rocks (Abdallah, 2007)

In water-wet pores, the rock surface is preferentially wetted by the water, so water will advance along the wall of the pore then displacing oil in front of it (fig 2.8.a). At some points, the neck connecting the oil in the pore with the remaining oil becomes unstable and snap off. Consequently a spherical oil globule trapped in the center of the pore. After the water front passing, the snap off oil becomes immobile, and the oil production gets to the plateau after water breakthrough. The snap off residual oil exists in two forms which are small spherical

globules in the center of the larger pores and the larger patches of oil extending over many pores and completely surrounded by the water. [8, 16, 20, 22,26, 30, 32]

In a strongly oil-wet rock, the rock is preferentially in contact with the oil. Oil commonly will be found in the small pores and as a thin film on the rock surface, while water is located in the middle or center of the larger pores.

One of the first problems faced in trying to achieve representative wettability in laboratory core samples is to define what reservoir wettability is. There is no direct method of measuring reservoir wettability although interfaces can be drawn from core, tracer and log measurement.[7]

Experimentally in the laboratory 'wettability ' can be determined in a number of ways where historically there are two most common methods (the Amott and USMB methods). The Amott method consists of developing two wetting indices, where the water wetting index, WI, and the oil wetting index, OI. Mathematically the WI and the OI are shown in equation (2.1) and (2.2.).

$$WI = \frac{B1}{B1 + A2} \quad \text{(2.1)}$$

Where ;
WI = Water wetting Index
B1 = Area under the spontaneous imbibition curve,
A2 = Area under the forced imbibition curve,

$$OI = \frac{B2}{B2 + A1} \quad \text{(2.2)}$$

Where ;
OI = Oil wetting Index
B2 = Area under the spontaneous drainage curve,
A1 = Area under the secondary drainage curve.

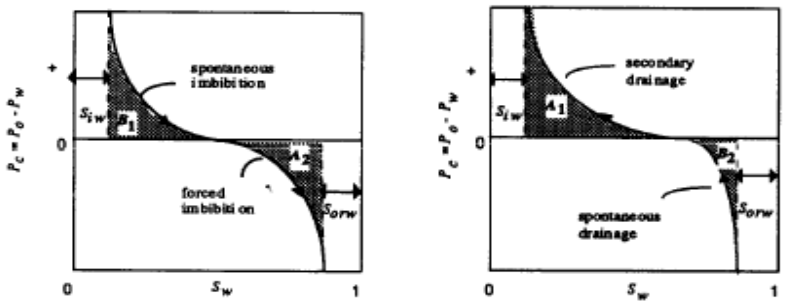

Fig 2.9. Illustration of the areas wettability index determination (Longeron, 1995).

The evaluation of reservoir wettability can be performed through measurement of IFT and the contact angle θ, (Ursin, 1997). This angle is defines as the tangent to the oil-water surface in the triple-point solid-water-oil, measured through the water phase (wetting phase) (Strand, 2005).

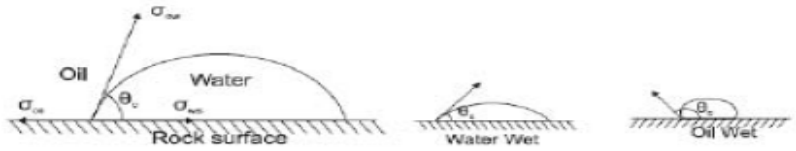

Fig 2.10. Measurement of the angle θ, through the water phase (Strand, 2005)

Table 2.1.Arbitrary wettability classes for a water-oil system (Ursin, 2000)

Wetting angle, θ	Wettability preference
0 - 30	Strongly water-wet
30 - 90	Preferentially water-wet
90	Neutral wettability
90 - 150	Preferentially oil-wet
150 - 180	Strongly oil-wet

2.5. Zeta Potential

From the theoretical point of view, zeta potential is electrical potential in the interfacial double layer (DL) at the location of the sipping plane versus a point in the bulk fluid away from the interface. In other words, zeta potential is the potential difference between the dispersion medium and the stationary layer of the fluid attached to the dispersed particle. The magnitude of the zeta potential is related to the surface charge at the oil/brine and mineral/brine interfaces, and the thickness of the double layer. Farooq et al. (2011) studied the effect of pH and ionicvalency (Na^{+}, Ca^{2+} and Mg^{2+}) on the zeta potential of different minerals and related it to surface charges. Zeta potential of Barea sandstone, silica, and kaolinite were highly negative in fresh water at pH>6, followed by NaCl solution, low salinity solution (1500 ppm) and solutions with diavalentcations. For all the minerals, it was found that Ca^{2+} and Mg^{2+} reduced the electropheric mobility and zeta potential more effectively than Na+ ions. Surface charges of sandstone and clay particles are significantly affected by ionic strength of water (Alotaibi et al. 2010). [16]

Rock wettability depends on stability of water film between rock surface and crude oil (Hirasaki 1991). The stability of water film is a function of the electrical double-layer repulsion that results from surface charges at the solid/water and water/oil interface. If this two interfaces have similar charges, a repulsive electrostatic force will occur that keeps the disjoining pressure high, and maintains a thick water film and consequently this produces a water-wet rock surface (Dubey and Doe 1993). Sandstone is negatively charged above pH=2 (Menezes et al. 1989). Polar components in the crude oil are positively at lower pH and negatively charged at higher pH. As the solution pH increases, oil charge deceases until reaches zero at the isoelectric point and becomes strongly negative. This positive-to-negative trend is seen with all oils, and it has been determined that the isoelectric point occurs at pH ranges from 2 to 6 based on the oil consumption (Takamura and Chow 1985; Buckley et al. 1989).

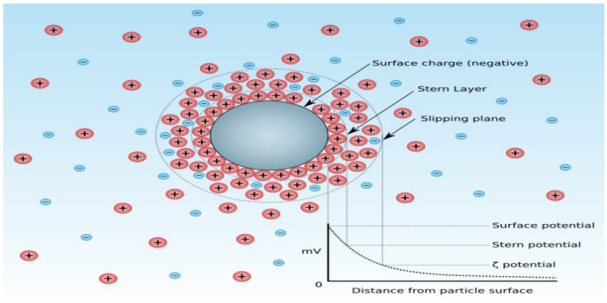

Fig 2.11. Zeta potential

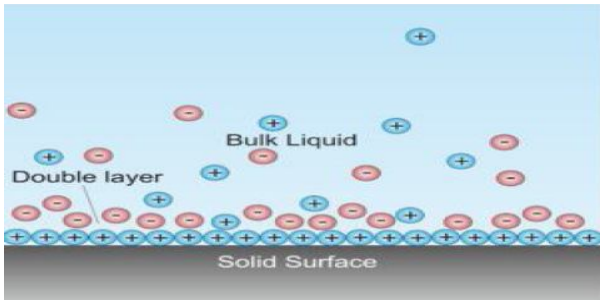

Fig 2.12. Schematic double layer in a liquid t contact with a negatively/charged solid.

2.6. Electrophoretic mobility

Electrophoresis is the motion of dispersed particles relative to a fluid under the influence of a spatially uniform electric field. This electro kinetic phenomena was observed first time in 1807 by Ferdinand Frederic Reuss (Moscow State University) who noticed that the application of a constant electric field caused clay particles dispersed in water to migrate. Electrophoresis of positively charged particles (cations) is called cataphores, while selectrophoresis of negatively charged (anions) is called anaphoresis.

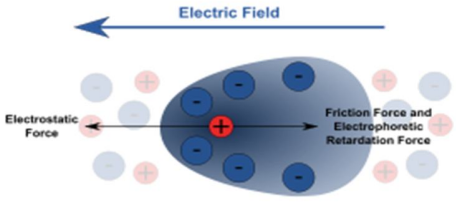

Fig 2.13. Illustration of electrophoresis

2.7. Displacement forces

An important aspect of any enhanced oil recovery process is the effectiveness ofthe process fluid in removing oil from the rock pores at the microscopic scale. Enhanced oil recovery processes typically involve the injection of multiple fluid slugs where the efficiency of these

fluids through the reservoir are the most of interest. Poor efficiency leads to an early deterioration and break down of the slugs which ends up of a poor project performance.[1, 2, 34]

2.7.1. Capillary Forces

In porous media capillary pressure is the force necessary to squeeze a hydrocarbon droplet through a pore throat (work against the interfacial tension between oil and water phase) and is higher for smaller pore diameter. The Yung – Laplace equation states that this pressure difference is proportional to the surface tension, δ, and inversely proportional to the effective radius, r, of the interface, and it also depends on the wetting angle, θ, of the liquid on the surface of the capillary.[1, 2, 34]

$$Pc = P_o - P_w = \frac{2\delta\cos\theta}{r} \quad \text{(2.3)}$$

Where,

Pc = capillary pressure, the equation for capillary pressure is valid under capillary equlibrium, which means that there can not be any flowing phase.
δ = interfacial tension (IFT)
θ = wetting phase angle
r = radius

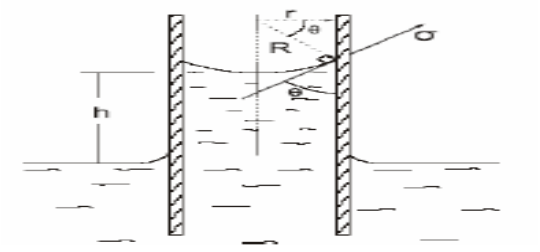

Fig 2.14. Use of capillary tube to measure capillary pressure (Strand, 2005)

The mathematical expression for Brooks-Corey capillary pressure model [2]. The Brooks-Corey capillary pressure model works satisfactorily in many cases and has been utilized widely for several decades in petroleum and other industries .[2]

$$Pcow = Pc(S_{wD})^{-\frac{1}{\lambda}} \quad \text{.....(2.4)}$$

Where λ is the pore size distribution index which is representation of the heterogenity , and Pc is the entry capillary pressure, and S_{wD} is the normalized saturation of the wetting phase and expressed as;

$$S_{wD} = \frac{Sw - Siw}{1 - Siw - Sor} \quad \text{... ... ... (2.5)}$$

Where Siw is the irreducible water saturation and Sor is the residual oil saturation.

Pooladi-Davish and Firoozabadi[2] presented another equation for capillary pressure as;

$$Pcow = PclnS_{wD}, \quad \text{... ... ... (2.6)}$$

Where $Pcow$ Is the capillary pressure constant, and S_{wD} is the normalized aturation of the wetting phase defined in Brooks-Corey equation.

Li[2] suggested the following capillary pressure model as described below;

$$Pcow = P_{max}(1 - bS_{wD})^{-\frac{1}{\lambda}} \quad \text{... ... ... (2.7)}$$

Where P_{max} is the capillary pressure at the residual non-wetting phase saturation the imbibitions case and the capillary pressure at the residual wetting case in the drainage case. b is a constant and expressed as;

$$b = 1 - (\frac{Pe}{P_{max}})^{-\lambda}, \quad \text{... ... ... (2.8)}$$

Where $\lambda = 3 - D_f$, and D_f is the fractal dimension, which is a representation of the heterogeneity of rock. For $D_f < 3$, if P_{max} approaches infinity, then Brooks-Corey's equation is valid for capillary pressure calculation.

2.7.1.1. Drainage and Imbibition Capillary Pressure.

They are two basic types of capillary pressure process (drainage and imbibition). By definition, the drainage process is the non-wetting fluid displaces the wetting fluid, while the imbibition is the contrary. To establish a drainage capillary pressure curve, the wetting-phase saturation is reduced from its maximum to the irreducible minimum by increasing the capillary pressure from zero to large positive value. To develop an imbibition capillary pressure curve, the wetting-phase saturation is increased. [2, 4]

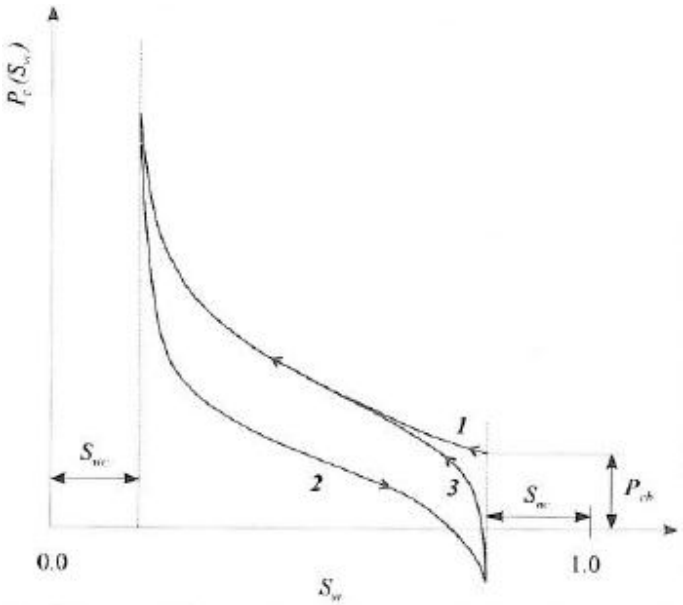

Fig 2.15. Typical of capillary pressure cure. (Ursin, 2000): (1). Primary Drainage, (2). Imbibition, (3). Secondary drainage.

2.7.2. Viscous forces

Viscous forces in a porous medium are reflected in the magnitude of the pressure drop that occurs as a result of flow of a fluid through the medium. One of the simplest approximation used to calculate the viscous forces is to consider a porous medium as a bundle of parallel capillary tubes.[1, 2, 4] Base on this assumption, the pressure drop from laminar flow through a single tube given by Poiseulle's law:

$$\Delta P = -\frac{8\mu L v}{g_c r^2} \quad \text{.....(2.9)}$$

Where

ΔP = pressure drop acroos the capillary tube
L = Capillary – tube lentgh
v = average velocity in the capillary tube
μ = viscosity of the flowing fluid
g_c = conversion factor

Viscous forces can be expressed in terms of Darcy's Law;

$$\Delta P = -(0.158)\left(\frac{\mu L v \emptyset}{k}\right) \quad \text{..... (2.10).}$$

Where
ΔP = pressure drop acroos the capillary tube, Psi
L = Capillary – tube lentgh, ft
v = average velocity in the capillary tube, ft/day
μ = viscosity of the flowing fluid, cp
∅ = porosity of the porous medium
k = permeability, darcies
And

$$k = 20 * 10^6 d^2 \emptyset \quad \text{..... (2.11)}$$

Where

∅ is the effective porosity of the bundle of the capillaries, and d is the diameter of the capillary tube.[1]

2.7.3. Gravity forces

There are mainly four factors that controlled primarily the vertical sweep efficiency in a reservoir such as; gravity segregation, mobility ratio, vertical to – horizontal permeability variation and capillary forces.

A gravity segregation occurs when the density difference between the injected and displaced fluid are large enough to induce a significant component of fluid in the vertical direction even when the principal direction of fluid is in the horizontal plane. When the density of injected

fluid is less than the displaced fluid, gravity segregation occurs and the displacing fluid overrides the displaced fluid(so-called gravity override) as shown in figure 2.16a. when the injected fluid is more dense than displaced fluid, a so-called gravity underside occurs as shown in figure 2.16b as for a waterflood.

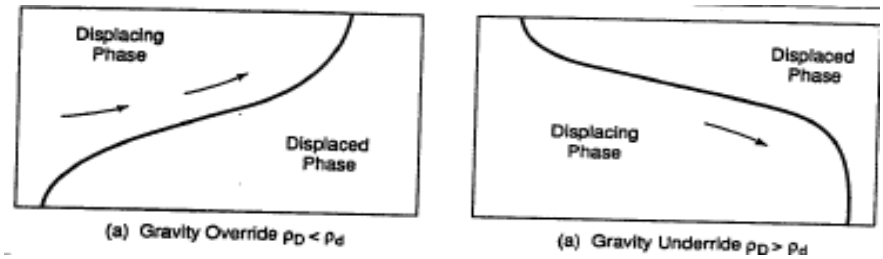

Fig 2.16. Gravity segregation in displacement process (Willhite, 1998).

Craig et al. studied vertical sweep efficiency by conducting a set of scaled experiments in linear system and five-spot models. Results of the linear displacements are shown in figure 2.17, where vertical sweep efficiency (EI) at breakthrough is given as function of a dimensionless group called a viscosity/gravity ratio.[1, 2, 8]

$$R_{v/g} = \left(\frac{\mu_d v}{kg\Delta\rho}\right)\left(\frac{L}{l}\right) \quad \text{(2.12)}$$

Where
μ = linear Darcy velocity,
μ_d = viscosity of displaced phase
$\Delta\rho$ = density difference
k = porous media permeability
L = lentgh of the system
h = heigth of the system

$$k = (k_v k_h)^{\frac{1}{2}} \quad \text{(2.13)}$$

The magnitude of viscous forces relative to gravity forces increases with increasing the $R_{v/g}$values. At small value of $R_{v/g}$ values, the displaced phase tends to override or underride, depending of the magnitude of the liquid densities, which leads to early breakthrough of displacing phase.

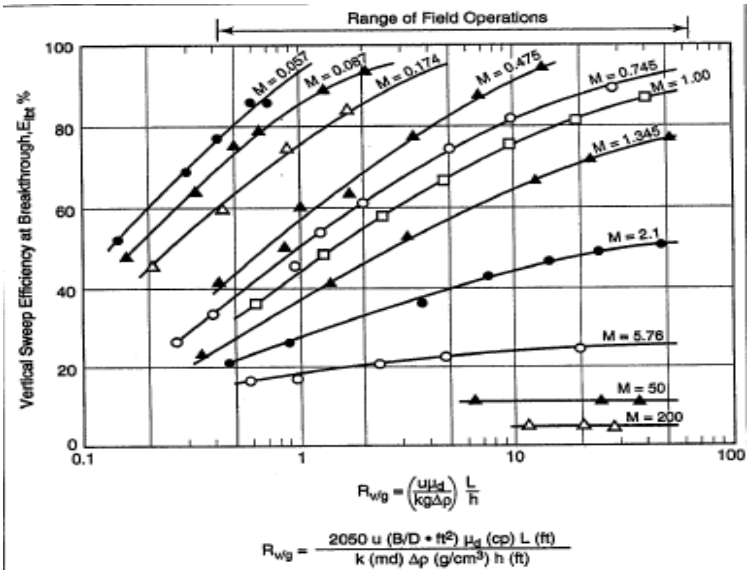

Fig 2.17. Volumetric (vertical) sweep efficiency at breakthrough as a function of the ratios of viscous/gravity forces, linear system ((Willhite, 1998).

2.8. Condition for low salinity effects

The listed conditions for low salinity effects are mostly related to the systematic experimental work by Tang and Morrow (199a), and from the work done by BP researchers (larger et al., 2007; Larger et al., 2008a).[5]

- Porous medium
  - Sandstones.
    - Low salinity effects have not been documented in pure carbonates, but Put et al., have observed effects in a sandstone containing dolomite crystal (Put et al., 2008).
  - Clay must be present
    - The type of clay may play a role.

- Oil
  - Must contain polar components (i.e. acids and base number).
  - Mineral oils
    - ➢ No effects have been observed.
- Formation brine
  - Formation water must contain diavalent cations, i.e. Ca^{2+}, Mg^{2+}, (Larger et al., 2008a).
  - Initial water must be present.
  - Efficiency is related to initial water saturation Swi.
- Low salinity injection fluid
  - The salinity is usually between 1000 – 2000 ppm, but effects have been observed up to 5000 ppm.
  - Appears to be sensitive to ionic composition (Ca^{2+}vs Na^{+},)
- Produced water
  - From a non-buffered system, the pH of the effluent water usually increase about 1-3 pH units when injecting the low salinity fluid.
  - It has not been verified that increase in pH is needed to observe low salinity effects.
  - In some cases, production of fines have been detected, but low salinity effects have also been observed without visible production of fines (Larger et al., 2008a).
- Permeability decrease
  - Usually an increase in pressure over the core is detected when switching to the low salinity fluid, which may be related to migration of fines formation of an oil/water emulsion.
  - There is lack of experimental evidence to say that observed low salinity effects are accompanied by permeability reduction.

- Waterflood experiments have been performed without any variation in end point relative permeability data between high and low salinity waterflood, under both secondary and tertiary flood conditions (Webb et al., 2008).

- Temperature
  - There appears to be no temperature limitations to where low salinity effects can be observed. Most of the reported studies have, however been performed at temperature below 100^0C.

2.8.1. Different Alternative Low Salinity Mechanisms

There are several hypotheses have been proposed as the mechanism to contribute for a better oil recovery by using low salinity process. "Migration of fines" by Tang and Morrow 1999, "pH increase" by McGuire et al 2005., "Double layer effect" by Ligthelm et al 2009., "Multicomponent Ionic Exchange"(MIE) by Larger et al 2006,. However so far none of these mechanisms have commonly been accepted and being agreed as the main contributor to the observed Low Sal effect.[5]

2.8.2. Migration of fines

Fines migration are defined as of movement of fine clay, quartz particles or similar materials within the reservoir formation due to drag force during production. Fine migration may result from an unconsolidated or inherently unstable formation, or from use of an incompatible fluid that liberates fine particles. Fines migrations causes particles suspended in the produced fluid to bridge the pore throats near the wellbore, and reducing well productivity.

The mobilization of fines with the injected flowing fluid could also associate with a permeability reduction and formation damage around the well bore due to plugging of pores.

Fines migration and subsequent reduction in permeability occurs during core flooding experiments due to decreased water salinity, and increased flow velocity and altered water pH or temperature (Mugan, 1965; Bernard, 1967; Lever and Dawe, 1984; Valdya and Fogler, 1998. Civan, 2010).

Tang and Morrow (1999) reported that when injecting low salinity brine into Barea Cores, a sharp increase in pressure drop across the core was observed. At the collected effluent samples, they found small amount of solid particles, so called fines which mainly consisted of kaolinite clay fragments.[9]

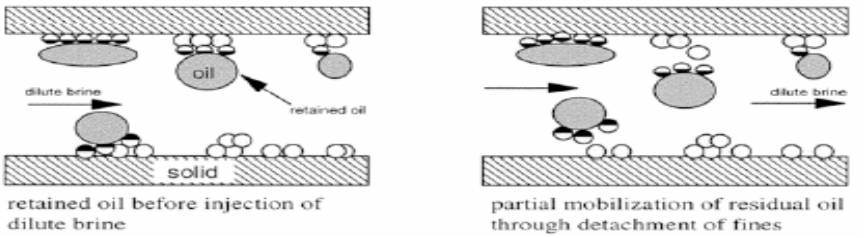

Fig 2.18. detachment of clay particles and mobilization of oil (Tang 1998)

2.8.3. pH increase

Since Morrow et al. progressed the research on the impact of brine salinity on oil recovery, researchers at the BP started evaluating the application of low salinity water flooding in the field, Webb et al. (2004) performed a logic-inject- log field test in Middle East to determine residual oil saturation to both high and low salinity water. There were three different brines of salinities 220,000 ppm, 170,000 ppm, and 3,000 being injected into the reservoir from a producing well, and the results showed that injecting low salinity water giving a significant reduced remaining oil saturation in the near well bore region. McGuire et al.(2005) suggested that the low salinity effect could be related to a type of alkaline waterflood, and at pH above 9 the flooding process would be equivalent to an alkaline flood. At high pH the acid compounds in the crude oil behaves as surfactants (Boussour, 2009). McGuire et al. also suggested that a

higher pH can increase the oil recovery by generation of surfactants and reduction of interfacial tension. The observed increase in pH is caused by formation of excess hydroxyl ions, OH^-, due to two different mechanisms which are mineral dissolution and ion exchange (Austad et al., 2010; Larger et al., 2006; McGuire et al., 2005). Mineral dissolution, mainly of carbonate (calcite/dolomite), is a relatively slow process, while cations exchange between the brine and the clay surface is a faster mechanism where H^+ ions could exchange with cations adsorbed onto the clay. [5, 9]

Larger A. 2006, proposed that the increase in pH is due to the following chemical reaction;

- Cation exchange between clay minerals and invading water. The mineral surface will exchange H^+ present in the liquid phase with cation previously absorbed. This reaction Is relatively fast.
- Dissolution of carbonate (calcite and/or dolomite), which results in an increase of OH^- and increase in pH. This dissolution reaction is slower and dependent on the amount of carbonate material present in the rock, but also on the concentration of Ca2+ in the Formation Water/LS water due to common end effect.

$$CaCO_3 \leftrightarrow Ca^{2+} + CO3^{2-} \quad \text{.....(2.14)}$$

$$CO3^{2-} + H2O \leftrightarrow HCO_3^- + OH^- \quad \text{.....(1.15)}$$

2.8.4. Multicomponent Ion Exchange (MIE)

Larger et al. (2006) discussed the responsible mechanism for improvement of oil recovery by low salinity water flooding and they reported that multi-component ionic exchange between the mineral surface and the invading brine was the primary mechanism behind.The authors suggested that during aging process, crude oil can be attracted or adsorbed to the surface through specific interactions as illustrated in (fig 2.19). During a low salinity waterflood, the divalent cations could be exchanged by monovalent cations which no longer hold the oil to the surface. [9, 10]

Fig 2.19. Illustrated hematic of Oil & Ckay (Leigh et al. 2010)

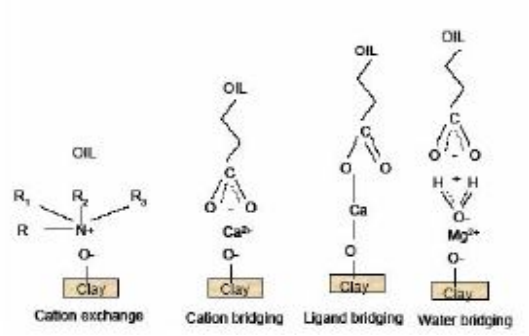

Fig 2.20. attraction between clay surface and crude oil by divalent cations (Larger A, 2008)

2.8.5. Chemical low salinity mechanism

Austad et al.(2010) carried out experiment on outcrops sandstones core plugs from a query in France, and based on the observations from these experiments proposed that the following parameters will play a major role in conditions for observing low salinity effects;[5, 9, 10]

- Clay properties/type and the amount present in the rock.
- Polar components in the crude oil, both acidic and basic.
- The initial formation brine composition and pH.
- It is further assumed that EOR effects of low salinity flooding is caused by improved water wetness of the clay minerals present in the rock.

Initially, both basic and acidic organic materials are absorbed onto the clay surface together with inorganic cations, specially Ca^{2+}, from the formation water. A chemical equilibrium is then established at actual reservoir conditions such as pH, temperature, and pressure etc. It is important to remember that the initial pH of the reservoir formation water may be even below 5 due to dissolved CO_2 and H_2S.

When the low salinity water is injected into the reservoir with an ion concentration much lower than that initial formation brine, the equilibrium associated with the rock-brine interaction is disturbed, and a net desorption of cations, especially Ca^{2+} occurs. In order to compensate for the loss of cations, then proton, H^+ from the water close to the clay surface adsorbs onto the clay, and consequently a substitution of Ca^{2+} by H^+ is taking palace.

The increase of pH close to the surface of the clay is illustrated in the equations below;

$$Clay\text{-}Ca^{2+} + H_2O \leftrightarrow Clay\text{-}H^+ + Ca^{2+} + OH^- \quad \text{.....(2.16)}$$

The local increase in pH close to the clay surface causes reactions between the adsorbed protonated basic and acidic material as in an ordinary acid-base proton transfer reaction, as shown in the equation below;

$$Clay\text{-}NHR_3^+ + OH^- \leftrightarrow Clay + R_3N + H_2O \quad \text{.....(2.17)}$$

$$Clay\text{–}ROOH + OH^- \leftrightarrow Clay + RCOO^- + H_2O \quad \text{.....(2.18)}$$

The adsorption of basic materials onto clay minerals is very sensitive to change in pH. Thus desorption of initially adsorbed cations from the clay is the key process in increasing the pH of the water that is localized close to the clay surface.

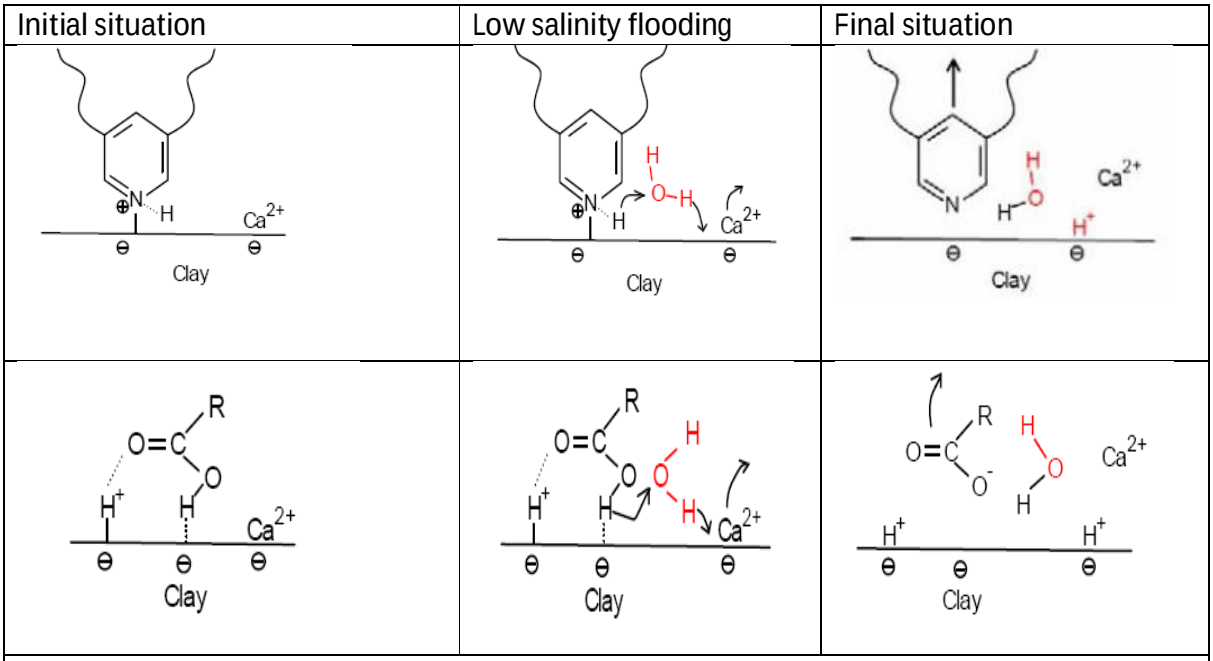

Fig 2.21. proposed mechanism for low salinity EOR effects. The initial pH at reservoir condition~ 5 ppm (Austad, 2010b). Upper: desorption of basic material.
Lower: desorption of acidic material.

2.8.6. Clay properties/type and the amount present in the rock

The crystal structure of common sandstone reservoir clays is made up of sheets of tetrahedral silica and octahedral aluminum layers. The presence of active clay minerals is essentially required to obtain low salinity effect. Thee clays are often characterized as cation exchange material, due to the structure charge imbalance, either in the silica or in the aluminum layer and also at the edge surfaces, causing a negative charge on the clay surface. The relative replacing power of cations is commonly believed to be:[5, 9, 10]

$Li^+ < Na^+ < K^+ < Mg^{2+} < Ca^{2+} < H^+$ ..... (2.19)

At equal concentration, Ca^{2+} will displace Na^{+} and vice versa. It is also important to note that the proton H^{+}, has the strongest affinity towards the clay surface. However the concentration of H^{+} is normally much lower than the concentration of cations present in the formation water at pH= 4-5. The magnitude of the selectivity of different cations towards different clays varies considerably (Kleven and Alstad 1996).

2.8.7. Polar components present in crude oil

The polar components in the crude oil which are more suitable to absorb onto reservoir minerals, are believed to be acidic or basic components. The acids are often termed naphthenic acids, in which the carboxylic group is part of large molecules that mostly are presented in the resin and asphaltene fraction. There are also fatty acids present in the crude oil. As it was reported by Havre et al. (2003), that the organic naphthenic acids have pK values around 4.9.
When pH is equal to the pK value, the concentration of the disassociated anionic from and the non-disassociated acid is equal. Based on the characteristic in relation to condition, both the protonated base and the neutral form of the acid are able to absorb onto the negative charged reservoir minerals , and the relative adsorption characteristic is surely depending on the pH.[5,9,10]

2.8.8. Desorption by pH increase

Desorption of initially adsorbed cations onto the clay is the key process in increasing the pH of the brine at the clay surface (latest proposed Low sal mechanism by Austad et al.). This pH increase causes desorption of organic material form the surface by an acid-base interaction. The strong dependence of pH in relation to adsorption/desorption was confirmed by static adsorption studies of a model base on kaolinite (Puntervold, 2010). One of the main statement in his hypothesis is that a local increase in pH at the clay surface, promoted by desorption of cations, are necessary to release oil components from the rock and thus evidently seeing the Low Salinity effect. Both acidic and basic crude oil material are released from the surface as the pH is increased from 5 – 6 to about 8 – 9 (Austad, 2010b).

2.8.8.1. Adsorption of basic material, Quinoline

Quinoline is a heterocylic aromatic organic compound with chemical formula C_9H_7N. it is a colourless hygroscopic liquid with a strong odor. Quinoline is only soluble in cold water but dissolves readily in hot water and most organic solvents. The molecular weight is 129.161 g/mol, and with pKa=4.8, the quinolone is at equilibrium with half at protonated form and half is in neutral form (Viswanath, 1979).

The concentration of two forms of quinoline is highly dependent on the pH in the solution, where the pH in the solution increased, the protonated form of quinoline is decreased.[17]

$C_9H_7N + H^+ \leftrightarrow C_9H_8N^+$ ..... (2.20)

pKa = 4.85

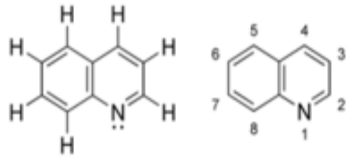

Fig 2.22. Quinoline

The adsorption of the base quinolone onto kaolinite and montmorillonite versus variation in pH can be seen in the fig 2.23. The adsorption decreases as pH increases. Low Salinity oil recovery test in lab experiments, an increase in pH is usually verified. However due to the buffering effects at field conditions (CO_2 and H_2S), an increase in pH is seldom observed in the produced water (Putervold, 2010).

Kaolinite	Mountmorillonite
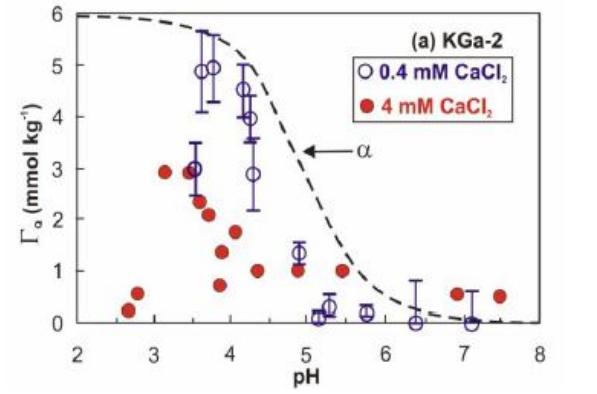	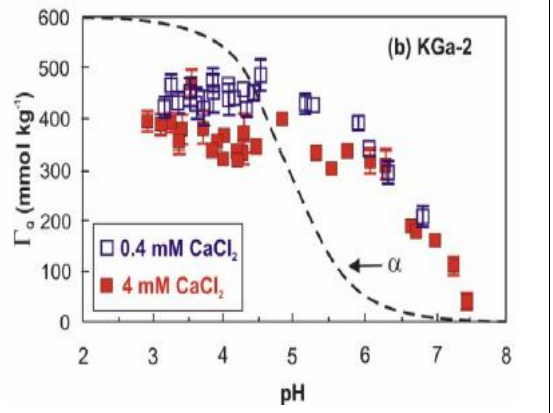

Fig 2.23. adsorption of quinolone onto kaolinite and montmorillonite (Burgos, 2002).

2.8.8.2. Adsorption of basic material, Quinoline onto illite

It was reported by Strand et al. that the adsorption of quinoline onto the illite at LS (1000 ppm) and HS (25000 ppm) brine at ambient temperature. The results showing that the highest adsorption close to pKa value and decreased adsorption at increased pH. And compared to the HS brine (fig 2.24) the LS brine has higher adsorption (Lower water-wetness).[17]

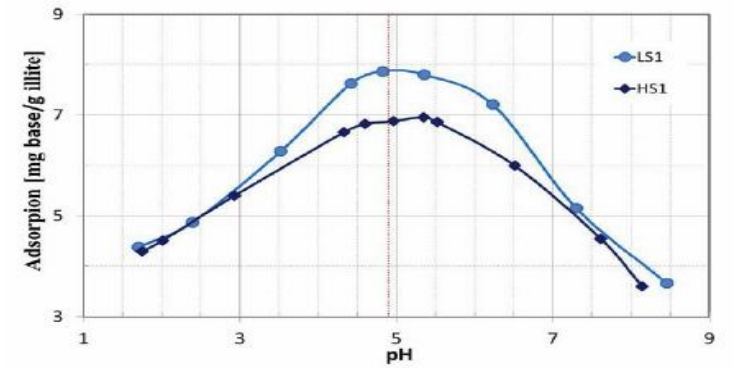

Fig 2.24. adsorption of quinoline onto illite at ambient temperature.

This confirms that the wettability alteration toward a more water-wet condition due to the decrease in salinity, but have to be linked to the pH increase close to the clay surface.

2.8.8.3. Deposit of asphalthenic crude oil onto kaolinite surface

The results observed with absorption of quinoline on illite clay has been confirmed using an alphatenic crude oil. Fogden and Labedeva, (SCA 2011) observed less deposits onto kaolinite clay with increasing pH and highest deposits occurred with LS-brine flooding (fig 2.25).[17]

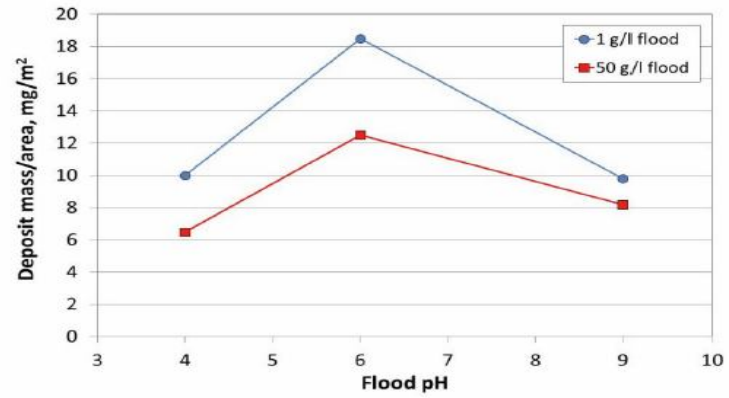

Fig 2.25. adsorption of crude oil onto kaolinite clays (SCA 2011)

CHAPTER III
EXPERIMENTAL WORK

3. Experimental and materials

Experimental work was performed on a reservoir system delivered by an oil company. The crude oil, 3 preserved cores and FW, SW and LS brine were used.

3.1. Crude oil and the measurements

Stabilized reservoir crude oil from an oil reservoir was used in these lab experiments. The crude oil was centrifuged to remove solid particles and water brines. Then the oil was filtered through a 5.0 µm filter paper (with a vacuum pump) to remove any dispersed particles in the crude oil.

3.1.1. Centrifuging and filtration process of crude oil

The IEC Model 2K-Centrifuge was used in this experiment. The crude oil sample delivered from the field was firstly poured in 2 one-litre container with equal weight placed in the centrifuge as shown in figure 3.1.a. The crude oil was separated from brine and particles by centrifuge forces at 90% of full speed.

The oil then was filtered with 5.0 µm Millipore SM filter and then the oil was stored in a sealed container. The centrifuge and filtration process as shown in fig 3.1a, 3.1b and 3.1c.

Fig 3.1.a. Centrifuge oil holder

Fig 3.1.b. speed regulator of centrifuge speed

Fig 3.1.c. Crude oil was filtered by 5.0 µm filter paper

3.1.2. Asphaltene

The amount of asphaltene was measured based on a modified ASTM method proposed by J. Buckley:

a. 1 ml of oil was accurately poured into a flask.

b. 40 ml heptane was added to the flask. Flask was sealed and shaken.

c. Mixture was aged for two days at ambient conditions and during this period, flask was shaken twice a day.

d. After ageing for two days, the mixture was filtered with a 0.22 µm pore filter paper.

e. Then, the filter paper was placed at 50°C oven and dried to constant weight.

f. By having the pre-weigh and weigh of filter paper after filtration process, the amount of asphaltene was calculated by the following formula.

$$\text{Asphaltene content } \left({}^{g}/_{100\ ml}\right) = \frac{\text{Weight of dried asphaltene (g)}}{\text{Volume of crude oil (ml)}} \text{x100} \ldots\ldots\ldots\ldots\ldots (3.1)$$

3.1.3. Acid number, AN

The Acid Number (AN) was determined by a Pothentemetric Titration. The used method was developed by Fan and Buckley (2006) and is a modified version of ASTM D664.

3.1.4. Base number, BN:

The Acid Number (AN) was determined by a Pothentemetric Titration. The used method was developed by Fan and Buckley (2006) and is a modified version of ASTM D664.

Table 3.1.the crude oil properties of Taqa field

	AN (20^0C) [mg KOH/g]	BN (20^0C) [mg KOH/g]	Asphaltene [g/100ml]	Density g/cm^3@ 20^0C	Viscosity [cp] @ 20^0C
Crude Oil	0.0	1.35	0.57	0.847	Not Measured

3.2. Brines

The brine composition used in these experiments was delivered by the oil company such as Formation Water (FW), Sea Water (SW) and Low Sal (LS). The brines were prepared by dissolving the reagent grade salts in distilled water . The solutions were stirred with a magnetic stirrer as shown in figure 3.3. All the brines were filtered through a 0.22 µm filter as to remove any particles, prior to the experiments.

Fig 3.2. Low Sal preparation

3.2.1. Density.

The density of oil and brines was measured by using AntonPaar DMA 4500 Density meter. The measurement was performed at 20^0C. Prior to the test, the U-tube was cleaned with white spirit and acetone. The white spirit removed the oil while acetone absorbed water and dissolved the white spirit. It is important to avoid gas bubble entering the tube during the sample injection for the density measurement , otherwise accuracy will not be obtained.

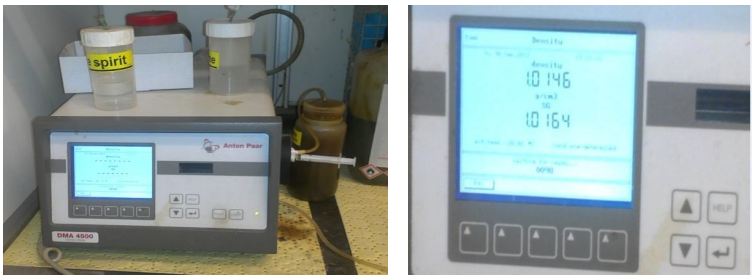

Fig 3.3. Anton Paar DMA 4500 Density meter.

Table 3.2. showing the properties of the brines at 20^{0}C, and the density of the Formation Water (FW), Sea Water (SW) and Low Sal (LS).

Table 3.2.Brine compositions

SALT	FW		SW		LS	
	m[g/l]	mMole/liter [molar]	m[g/l]	mMole/liter [molar]	m[g/l]	mMole/liter [molar]
SSW	22.11		38.67		1.94	
NaCl	21.52	0.368	23.38	0.400	0.90	0.015
Na2SO4	0.00	0.000	3.41	0.024	0.12	0.001
KSCN	0.00	0.000		0.000	0.00	0.000
NaHCO3	0.23	0.003	0.17	0.002	0.00	0.000
KCl	0.23	0.003	0.00	0.00	0.03	0.000
AlC3	0.00	0.000				
MgCl2 x 6H20	0.28	0.001	9.05	0.045	0.36	0.002
CaCl2 x 2H2O	0.51	0.003	1.91	0.013	0.05	0.000
BaCl2 x 2H2O	0.15	0.001	0.00	0.00	0.00	0.000
SrCl2 x 2H2O	0.23	0.001	0.00	0.00	0.00	0.000
IONS	**m[g/l]**	**mMole/liter [molar]**	**m[g/l]**	**mMole/liter [molar]**	**m[g/l]**	**mMole/liter [molar]**
HCO_3^-	165.6	2.7	123.5	2.0	0.0	0.0
Cl^-	13625.5	384.0	18617.4	525.1	705.5	19.9
SO_4^{2-}	0.0	0.00	2306.0	24.0	78.4	0.8
SCN^-	0.0	0.0	0.0	0.0	0.0	0.0
Mg^{2+}	34.0	1.4	1082.4	44.5	42.9	1.8
Ca^{2+}	140.1	3.5	520.0	13.0	12.6	0.3
Na^+	8527.6	370.9	10347.4	450.1	390.8	17.0
K^+	120.1	3.1	393.5	10.1	14.7	0.4
Ba^{2+}	84.1	0.6	0.0	0.0	0.0	0.0
Sr^{2+}	76.0	0.9	0.0	0.0	0.0	0.0
Al^{3+}	0.0	0.0	0.0	.0	0.0	0.0
TDS, g/l		222.19	33390.0	33.43	1245.0	

3.2.2. Calculation of effluent salinity

By knowing the density of the reservoir FW and distilled water were used, the salinity of the mixture at the effluent can be determined by using a linear equations as following;

$$TDS_e = TDS_{FW} - \frac{\rho_{WF} - \rho_e}{\rho_{WF} - \rho_{DW}} * TDS_{FW} \quad \ldots\ldots (3.2)$$

Where:

TDS_e = Total disolved solid of effluent brine [ppm]

TDS_{FW} = Total disolved solid of formation water [ppm]

ρ_{WF} = Density of FW $[\frac{g}{cm^3}]$

ρ_e = Density of effluent brine $[\frac{g}{cm^3}]$

ρ_{DW} = Density of destilled water $[\frac{g}{cm^3}]$

3.3. Reservoir Cores

Three preserved reservoir cores (core#15, core#48 and core#60) were received from the oil company. The reservoir cores have the XRD analysis of clay content which showing an average clay content of 8 – 12%, where 2 – 4% of illite and 6 – 8% of kaolinite.

Table 3.3. XRD Analysis of Clay Content (data from the field)

Core#	Kaolinite	Illite
Core#15	6 – 8%	2 – 4%
Core#48		
Core#60		

Table 3.4. Core Properties

core	Cleaning	L [cm]	D [cm]	V_b [cm^3]	W_s [cm^3]	W_d [g]	W_f [g]	PV [cm^3]	Φ [%]	Swi [%]
Core# 15	Mild	5.07	3.79	57.19	128.50	117.77	119.94	10.714	0.187	20
Core# 60	Tol+MeOH	5.05	3.83	58.18	136.19	124.35	126.71	11.622	0.199	20
Core# 48	Tol+MeOH	5.07	3.78	56.89	135.27	125.93	119.94	9.208	0.16	20

Where:

L= Length of core

D= Diameter of core

V_b= Bulk volume of core

W_s= Weight of core 100% saturated with diluted FW

W_d= Weight of dry core

W_f = Final weight of core @ initial FW saturated after desiccators (desired weight)

PV= Pore volume of core

Φ = porosity of core

K= Permeability

Swi = Initial water saturation

3.3.1. Core cleaning

Core#15 was mildly cleaned while core#48 and core#60 were cleaned by Tol + MeOH.

3.3.1.1. Mildly cleaning

The core was inserted in a rubber sleeve and installed in a Hassler core holder with a confining pressure of 20 bar. Under mildly cleaning, the core was firstly flooded with kerosene until clear effluent was observed. Then the core was flooded with heptane to displace the kerosene fraction. The core was then placed in a heating oven at 90^0C until a constant weight.

Fig 3.4. Mildly cleaning core set up

3.3.1.2. Toluene + Methanol cleaning

The core was inserted in a rubber sleeve and installed into Hassler core holder with a confining pressure of 20 bar. First, the core was flooded with Toluene until clear effluent was observed. Then it was flooded with Methanol. The core was then placed in a heating oven at 90^0C until a constant weight.

Fig 3.5. Toluene + Methanol cleaning core set up

3.3.2. Water saturation

The cleaned and dried core was weighted prior to the test. The cleaned an dried core was evacuated with a vacuum pump. As soon the pressure gauge was at a stable lowest value, the brine was introduced into the container to saturate the core. Then the weight of the saturated core could then be measured.

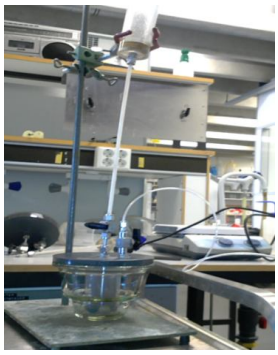

Fig 3.6. Saturation of core under vacuum pressure

3.3.3. PV measurement

The dry weight of the core was taken(dried at 90^0C) and recorded. Then the core was saturated with Formation water (FW) under vacuum condition. The pore volume was calculated as follow;

$$\text{Pore volume (ml)} = \frac{\text{Weight of 100\% saturated core (g) - Weight of dried core (g)}}{\text{Density of liquid } (^{g}/_{ml})} \ldots\ldots. (3.3)$$

3.3.4. Porosity measurement

The porosity of the core was obtained by using the flowing equation

$$\text{Porosity (\%)} = \frac{\text{Pore volume of the core (ml)}}{\text{Bulk volume of the core (ml)}} \text{x}100 \ldots\ldots (3.4)$$

3.4. pH Screening test

The core was 100% saturated with Formation Water (FW), inserted into the rubber sleeve, and installed it in the Hassler core holder. A confining pressure of 20 bar was applied.

The core was flooded at reservoir temperature with a rate of 4PV/D. A back pressure of 10 bar was maintained during the experiment. Effluent samples were collected in sealed glass containers for pH, density and ion concentrations analysis.

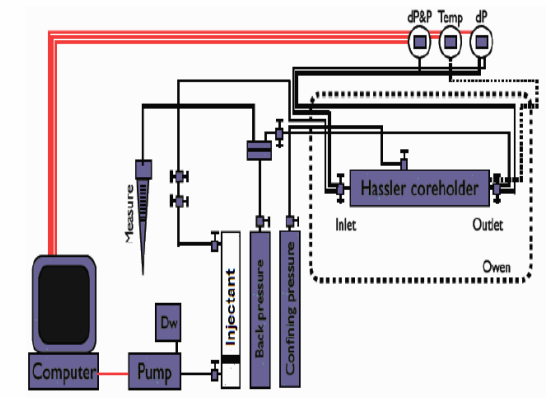

Fig 3.7(a). Apparatus for pH Scanning Waterflooding Test. The injectant cells consist of Formation Water , Sea Water and Low Sal cell.

Fig 3.7(b). pH scanning effluent samples collector

3.4.1. pH measurement

The effluent were collected into sealed samples glasses. The pH of the effluent was measured using a Mettler Toledo Seven Easy pH instrument as figure 3.8. Before carrying out the pH measurement, the probe was calibrated using buffer solutions with pH 4.00, pH 7.00, and pH 10.00. The calibration was carried out every time before a new sample series to ensure that the pH reading obtained was accurate.

Fig 3.8. Seven Easy pH measurement instrument

3.4.2. Chemical Analysis

The Dionex ICS-300 Ion chromatography (IC) was used for measuring the ion composition in the brine samples. In order to be within the optimal detection range for the IC, the brine samples were diluted to an expected ion concentration of ~0.5 mM, and filtered through a 0.2µm filter.

The brines sample of Low Salinity flooding were diluted with Deionized water 50 times (1:50) while Formation water and Sea Water were diluted 200 times (1:200) using CX – 271 LIQUID HADLER Instrument. After the brines were diluted and filtrated, the samples were poured into sealed HPLC sample bottles and placed in the IC Auto Sampler.

Sea Water brine samples where diluted 200 times and used as external standard for concentration calculations.

Fig 3.9 (a) CX-271 Liquid Hadler

Fig3.9 (b) Dianex ICS 3000

Fig 3.9 (c) An-Ion & Cat-Ion Display

3.5. Core Restoration

3.5.1. Establishment of initial water Saturation using the desiccator technique

An initial water saturation of 20% was established in the core . It is assumed that this value is below the irreducible water saturation at the reservoir condition, and thus water saturation will not be changed or moved during the primary drainage. The core was saturated with 5 times diluted FW.

The core was placed into the desiccator on a frame with silica gel at the bottom of the desiccator. The silica will absorb water from the core until the desired weight that corresponding to the initial water saturation (20%) was obtained. The weight of the core was measured frequently until the final desired weight was reached, approximately after two days. The desired weight of the core can be calculated by using the following formula (equation 3.5).

$$W_f = W_d + (0.20*PV*\rho_{fw}) \quad \text{.....(3.5)}$$

Where:

W_f= desired weight at 20% water saturation [g]

W_d = weight of dry core, [g]

PV = Core Pore Volume [cm^3]

ρ_{fw} = density of the formation water [g/cm^3]

After obtaining the initial water saturation, then the core was stored in a sealed container at ambient temperature for three days to equilibrate the initial water saturation of the core.

Fig 3.10. Establishment of initial water saturation using desiccator

3.5.2. Oil saturation

The initially saturated core was vacuumed with the vacuum pump at about 10 mint as to imbibe the oil into the core.

The core (initially Swi=20%) was installed in a rubber sleeve and mounted into the Hassler core holder. A confining pressure of 20 was applied. Then the core was flooded with crude oil from both sides. Inlet and the outlet lines and the core was connected to a vacuum pump for a short time.

The temperature was increased to 50^0C, and then the core was flooded 2 PV with crude oil in each direction with a rate of 0.1 ml/min.

Fig 3.11. Hassler Core Holder

3.5.3. Ageing of Core

The saturated and flooded core was wrapped with Teflon to avoid unrepresentative wetting on the core surface. The core was placed and surrounded by crude oil in a steel aging cell on marble balls. The cell was pressurized (10 bar) with crude oil at reservoir temperature for 14 days. The core in the aging cell can be seen in the fig 3.12

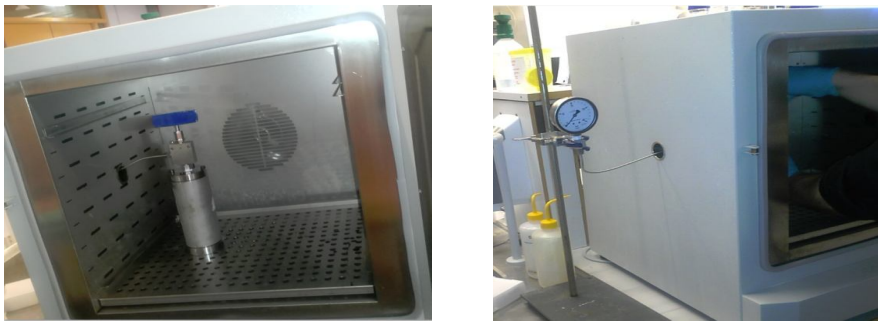

Fig 3.12. Aging core under reservoir temperature condition (130^0C)

3.5.4. Oi recovery test by Water flooding

The restored core (Swi = 20% and aged in crude oil) was inserted into the rubber sleeve, and installed into Hassler core holder. A confining pressure of 20 bar was applied during the experiment.

The core was successively flooded at reservoir temperature with FW-SW-LS brines at a rate of 4PV/D with a back pressure of 10 bar. The effluent brine were collected in a graded glass burette for oil recovery observation. During the waterflooding test, brine sample was taken frequently for pH and density measurement.

The recovery was calculated using the following equation:

$$R = \frac{V_{prod}}{OOIP} * 100 \ldots\ldots\ldots\ldots\ldots\ldots\ldots\ldots\ldots\ldots \quad (3.6)$$

Where:

R = oil recovery factor (%)

V_{prod}= Volume of Oil produced (ml)

OOIP = Original Oil In Place (ml)

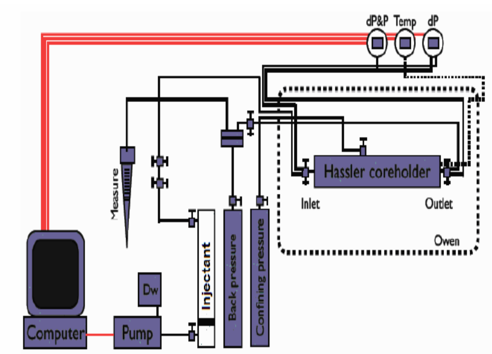

Fig 3.13 (a). Apparatus for Oil recovery Waterflooding Test. The injectant cells consist of Formation Water , Sea Water and Low Sal cell.

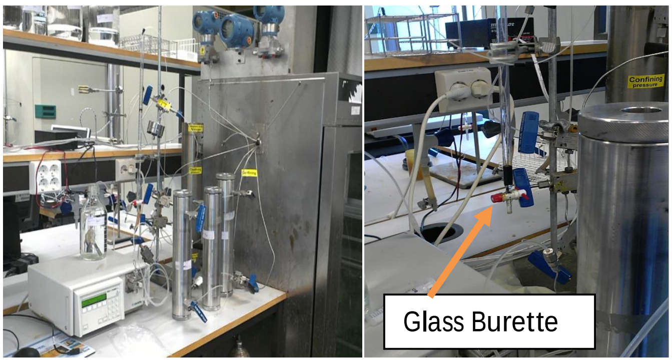

Fig 3.13 (b). Oil recovery experimental set up

CHAPTER IV

RESULTS

4.1. Introduction

The Low Salinity potential of a high temperature oil reservoir have been evaluated. The reservoir has already been flooded with sea water. The experiments have been performed on 3 preserved reservoir cores. We have also received stabilized crude oil from the reservoir. The oil company has also supported us with FW, SW, and a potential LS brine composition.

4.2. Crude oil properties

The evaluation of Low Salinity EOR potential are based on oil recovery tests, and pH scanning tests to observe pH changes in the effluent.

Stabilized reservoir crude oil from the reservoir was used in these lab experiments. The crude oil was centrifuged and filtered prior to use. AN, BN, Asphatene content and density were measured.

Table 4.1. Crude Oil properties (copied from page39)

	AN (mg KOH/g)	BN (mg KOH/g)	Asphaltene (g/100ml)	Density (g/cm^3) @ 20°C	Viscosity (cP) @ 20°C
Crude oil	0.0	1.35	0.57	0.847	Not measured

4.3. Core properties

The preserved cores (Core#15, Core#60 and core#48) were cleaned prior to use. PV was measured and porosity calculated. The core properties obtained as shown in table 3.2.

Table 4.2. Core Properties (copied from page 43)

core	Cleaning	PV[cm^3]	Φ[%]
Core# 15	Mild	10.71	0.187
Core #60	Tol + MeOH	11.62	0.199
Core #48	Tol + MeOH	9.208	0.16

Where:
PV= Pore volume of core
Φ = porosity of core

XRD analysis of clay content showed an average clay content of 8 – 12%, where 2 – 4% of illite and 6 – 8% of kaolinite.

Table 4.3. XRD Analysis of Clay Content (data from the field)(copied from page 42)

Core#	Kaolinite	Illite
Core#15	6 – 8%	2 – 4%
Core#48		
Core#60		

4.4. pH screening of core#60 at reservoir temperature; 130^{0}C

Core#60 was cleaned with Toluene + Methanol prior to use. The core was 100% saturated with FW and placed in the core holder with a confining pressure of 20 bar and back pressure of 10 bar. The core was heated to constant temperature of 130^{0}C during the night. Then the core was successively flooded with FW-SW-LS and FW with a constant rate of 4 PV/D at reservoir temperature of 130^{0}C. The pH, densityand ion concentration analysis of effluent samples were measured.The result s are presented in figure 4.1.

4.5. observation on pH screening of core#60

The pH gradually increased during FW flooding and stabilized at pH 7.3 after 30 PV of FW injected. Then the injection brine was switched to SW.The pH dropped to 6.6 and stabilizedafter 50 PV injected. When switching to Low Sal brine, the pH increased sharply and stabilized at pH 7.4, and then slightly decreased to 7.1 before switched back to FW after 60 PV injected.With FW, the pH rapidly decreased about 1 pH unit before it increased andstabilized at pH 7.3. Totally 77 PV was injected for the whole experiment.

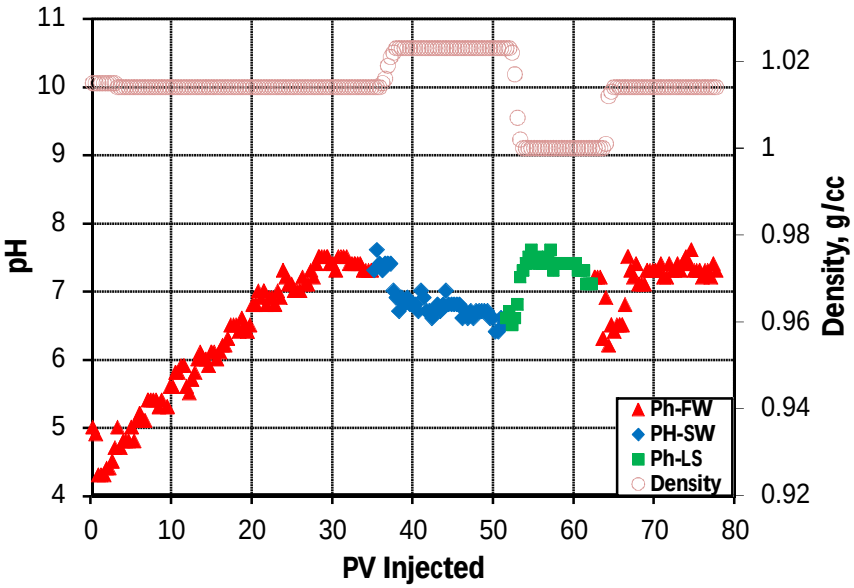

Fig 4.1.pHscreening of core#60, flooded with FW, SW and LS brine at 130^{0}C. The flooding was carried out at constant rate of 4PV/D with a backpressure of 10 bar.

4.6. Chemical analysis of effluent of core#60.

Before carrying out the chemical analysis the effluent samples with FW and SW were diluted 200 times with DI water and the samples with Low Sal brine were diluted 50 times. The results from the chemical analysis are presented in figure 4.2.

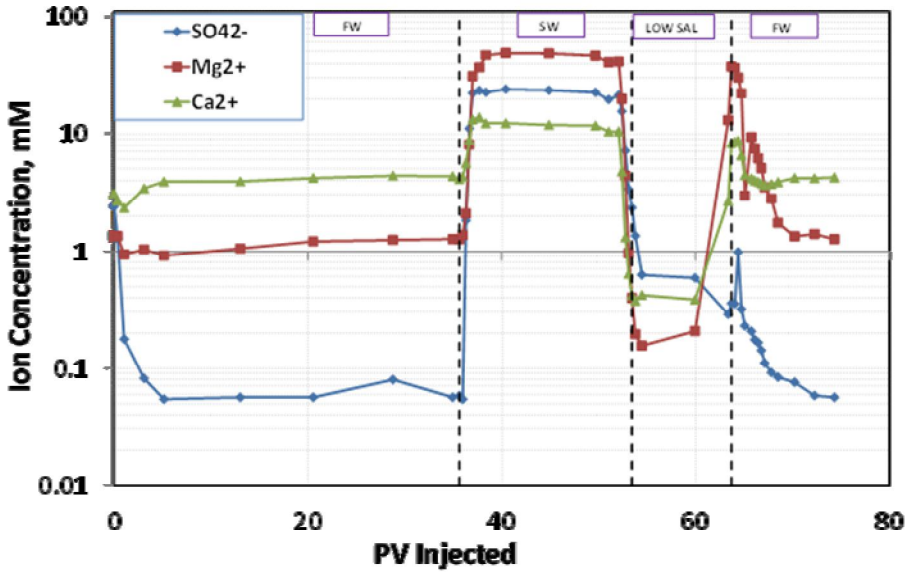

Fig 4.2.Chemical analyses of effluent from core #60, flooded with FW, SW and LS brine at 130 °C. The flooding was performed at constant rate of 4 PV/D with a back pressure of 10 bar.

During FW flooding the calcium concentration was initially at 3mM and stabilized at 4 mM.When SW was introduced, the calcium concentration increased and stabilized at 10.2mM.When we switched to LS the calcium concentration rapidly decreased to 0.3 mM.With FW, the calcium concentration again stabilized at 4 mM.

The magnesium concentration was initially at 1 mM and stabilized at about 1.2 mM during the formation water flooding. It increased rapidly to 40mM and stabilized at 45mM within the SW brine flooding. When switching toLS, the concentration of magnesium decreased and stabilized at about 0.2 mM. It peaked to 14mM (due to dilution effect from 50 times to 200 times on the switching period), and then back to initial condition when switched back to Formation Water.

The sulphate concentration was initially at about 1 mM and quickly decreased and stabilized at 0.05 mM within the Formation Water flooding. When switching to SW flooding, the sulphate concentrationincreased to 24 mM, equal to SW concentration.As the brine flooding was switched to Low Salinity (LS), the sulphate concentration stabilized at about 0.7 at the end of

the Low Sal phase flooding. When switching back to Formation Water brine the concentration of sulphate increased and stabilized at 0.05 mM till the end of flooding experiment.

4.7. pH screening of core#48 at reservoir temperature; 130^{0}C.

Core#48was cleaned with Toluene + Methanol prior to use. The core was 100% saturated with FW and placed in the core holder with a confining pressure of 20 bar and back pressure of 10 bar. The core was heated to constant temperature of 130^{0}C during the night. Then the core was successively flooded with FW-SW-LS and FW with a rate of 4 PV/D at reservoir temperature of 130^{0}C. The pH, density and ion concentration analysis of effluent samples were measured.

4.8. Observation pH screening on core#48.

The initial pH of core#48was 5.9, and then it gradually decreased and stabilized at pH 6 after 11 PV of Formation Water brine injected. When switching to SWthe pH gradually decreased to pH 5.5 after totally 20 PV injected.Introducing the Low Salinitybrine, the pH increased one pH unitand stabilized at 6.5 after 28 PV injected. When the brine was switched back to Formation Water,the pH was decreased sharply to pH 6, and then it increased and stabilized at pH 7 after 38 PV being injected. The result s are presented in figure 4.3.

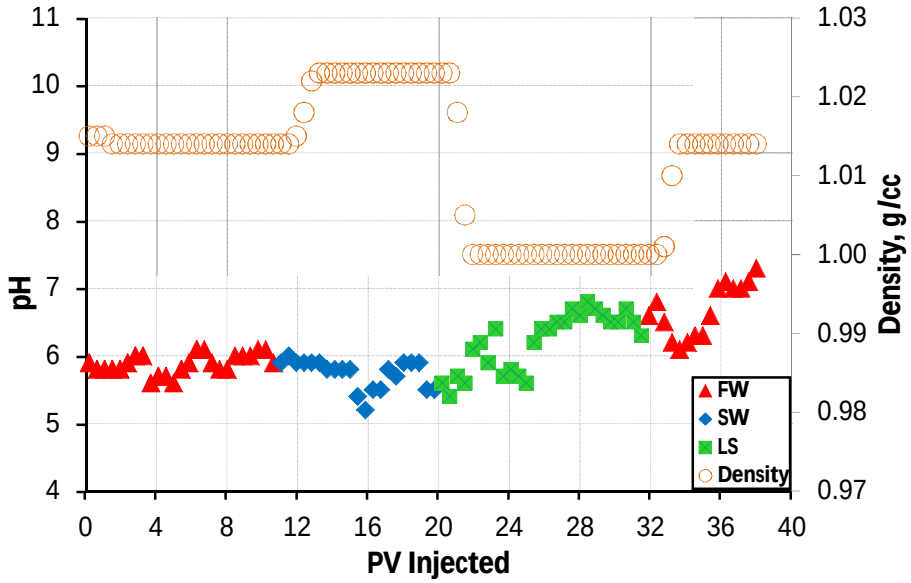

Fig 4.3.pH screening of core#48, flooded with FW, SW and LS brine at 96^{0}C. The flooding was carried out at constant rate of 4PV/D with a backpressure of 10 bar

4.9. Observation on Chemical analysis of effluent Pelican core#48 at 130^{0}C .

Before carrying out the chemical analysis the effluent samples with FW and SW were diluted 200 times with DI water. The samples with Low Sal brine were diluted 50 times. The results are presented in figure 4.4.

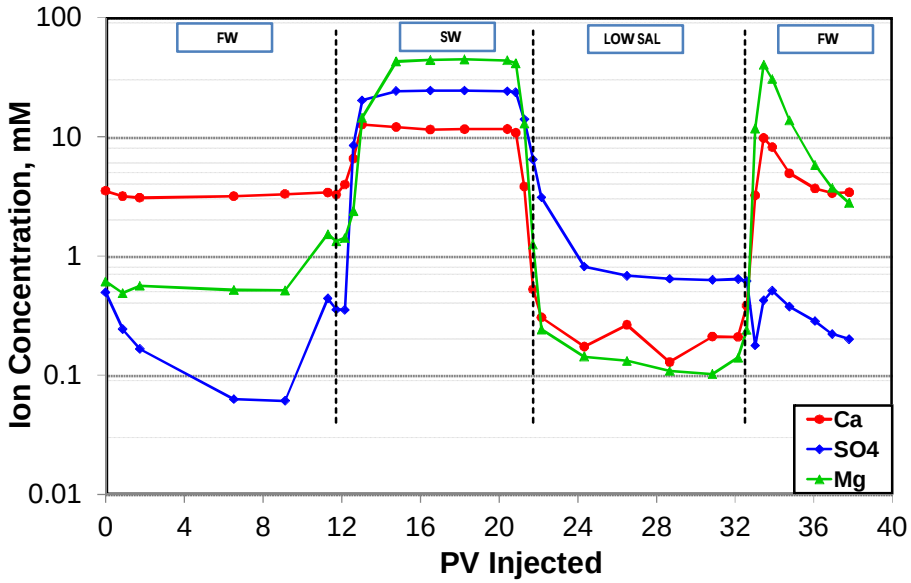

Fig 4.4. Chemical analyses of effluent from core #48, flooded with FW, SW and LS brine at 96 °C. The flooding was performed at constant rate of 4 PV/D with a Back pressure of 10 bar.

The calcium concentration was initially at 3.5mM and stabilized at 3.5mMduring the Formation Water flooding phase.The concentration increased to 10.2 mMduring SW brine flooding. When we switched to LS brine the calcium concentration decreased and stabilized at 0.2mM. When the brine was switched back to Formation Water, the calcium concentration increased (peaked at 10 mMdue to change in sample dissolution) and stabilized at 10 mM.

Themagnesium concentration was initially at 0.5 mMand decreased and stabilized at 0.06 mM during the formation water flooding.With SW, the Mgconcentration increased sharply and stabilized at 43.9mM. When we switched to Low Salinity brine, the concentration of magnesium decreased to0.24mM and stabilized at about 0.1 mM.When switching back to Formation Water, the ion concentration was increased to initial condition of the Formation Water.

The sulphate concentration was initially at about 0.5mM and slowlydecreased and stabilized at 0.06mM within the formation water flooding. The sulphate concentration was sharply increased and stabilized at 24.3 mM during SW flooding. When the brine was switched to Low

Salinity, the ion concentration decreased and stabilized at 0.64 mM.As the brine was switched back to Formation Water, thesulphate concentration dropped again.

4.10. Oil recovery tests

Oil recovery tests were performed on 2 cores. Core#15 was mildly cleaned before restoration. Core#60 was cleaned with Toluene and Methanol, and also was used in the pH screening test prior to restoration.

Both cores were restored with an initial FW saturation of 20%, saturated and aged with the crude oil at reservoir temperature of 130^0C.

The cores were successively flooded with FW-SW-LS with a rate of 4 PV/D at reservoir temperature of 130^0C .At the end the flow rate was increased to 16 PV/D to observe any end effects. The oil recovery was collected in a graded glass burette. The pH and density of produced brine were regularly measured during the water flooding .

4.11. oil recovery test on core #15

The core was successively flooded with FW-SW-LS with constant rate of 4 PV/D. At the end the flow rate was increased to 16 PV/D to observe any end effects. Figure 4.5 shows the oil recovery as a function of pore volume of brine injected.

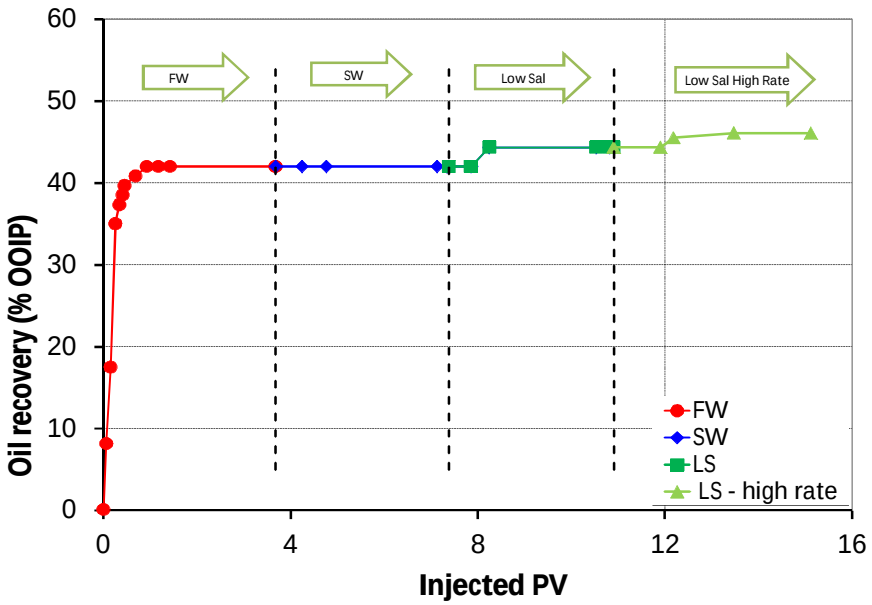

Figure 4.5. Oil recovery test of Pelican core # 15. The core was flooded with FW, SW and LS fluid at a rate of 4 PV/D. The oil recovery is plotted against PV injected. At the end the flooding rate was increased to 16 PV/D.

The recovery curve in figure 4.5 indicates a piston like displacement of oil until 35% oil recovery.Then both oil and water were produced. After 1.5 PV of brine injected, the oil production reached the plateau at 42% OOIP. After observingno oil recovered, the injection brine was switched to sea water. No increased oil recovery was observed during SW injection. Then weswitched to Low Sal brine. After 0.47PV injected, the oil recovery increased to 44.4%.The oil recovery then reminded constant. At the end, when the rate was increased to 16 PV/D, an oil recovery of 1.6% was observed after almost 1 PV being injected.

4.12 pH and density observation duringoil recovery test of core #15

The density of each fluid are in line with the expectations (FW = 1.014 g/ml, SW=1.023 g/ml, and LS= 1.000 g/ml). The results are presented in figure 4.6.

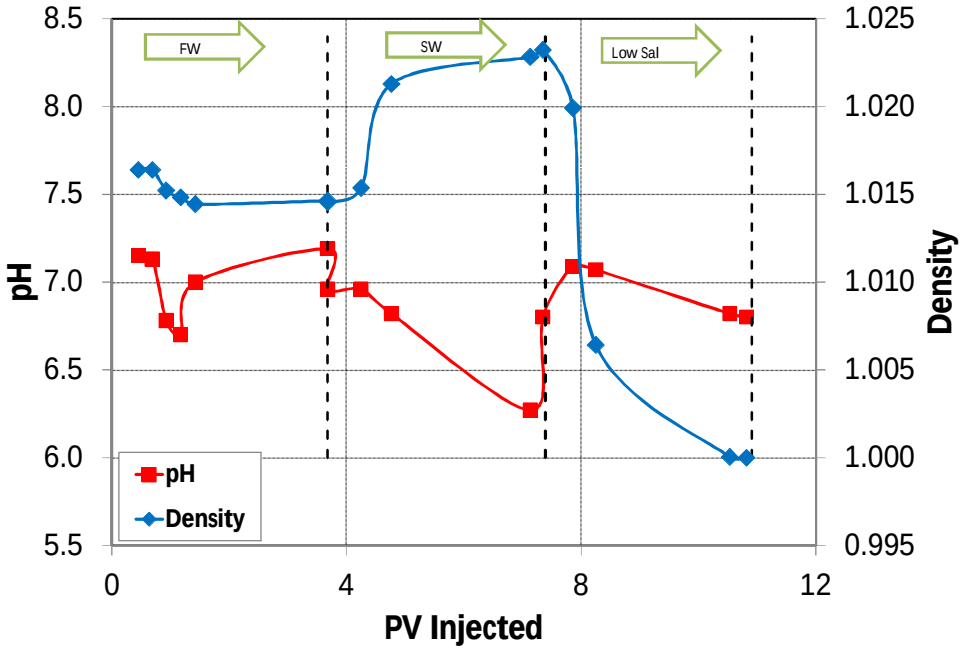

Figure 4.6. pH and Density as the function of PV injected on Oil recovery test of core #15. The core was flooded with FW, SW and LS fluid at a rate of 4 PV/D. The oil recovery is plotted against PV injected. At the end the flooding rate was increased to 16 PV/D.

During the FW flooding the density stabilized at ρ= 1.014 g/ml. During SW flooding the density was increased to ρ =1.023 g/ml. When switching to LS, the density was decreased to ρ=1.000 g/ml.

The pH results are somewhat fluctuating, but an initial pH down to 6.7 was observed. When switching to SW, the pH decreased down to 6.3. A rapid increase in pH up to 7.1 was observed when the LS brine was introduced, and then gradually decreased again.

4.13 oil recovery test on core #60

The restored core#60 was flooded with FW-SW-LS withconstant rate of 4 PV/D at reservoir temperature of 130^{0}C. At the end the flow rate was increased to 16 PV/D to observe any end effects. Figure 4.7 shows the oil recovery as a function of pore volume of brine injected.

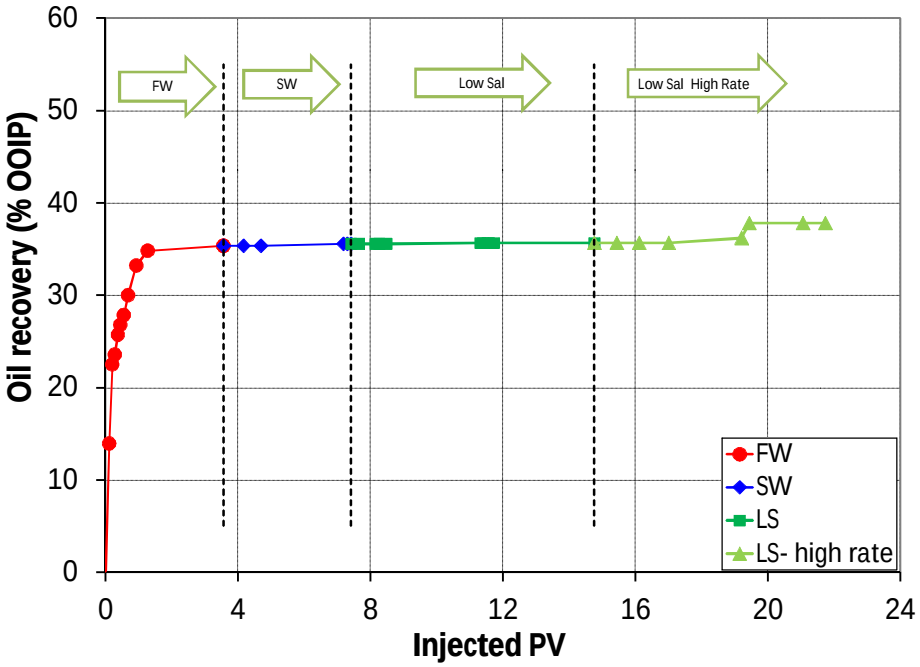

Figure 4.7. pH and Density as the function of PV injected on Oil recovery test core #60. The core was flooded with FW, SW and LS fluid at a rate of 4 PV/D. The oil recovery is plotted against PV injected. At the end the flooding rate was increased to 16 PV/D.

The recovery curve in figure 4.7shows a piston like displacement of oil until 25% recovery.Then both oil and water were produced. After 1.3 PV of brine injected, the oil production reached the plateau at 36.6% OOIP. After observingno more oil recovery, the injection brine was switched to sea water. No increased oil recovery was observed during SW injection. Thenwe switched to Low Salinity brine. Also there no increased oil recovery was observed. After totally 15 PV injected, the rate was increased to 16 PV/D. An increase in oil recovery of 1.2% was observed after 19 PV injected.

4.14. pH and density observation during oil recovery test on core #60

The density of each fluid are in line with the expectations (FW = 1.014 g/ml, SW=1.023 g/ml, and LS= 1.000 g/ml). The results are presented in figure 4.8.

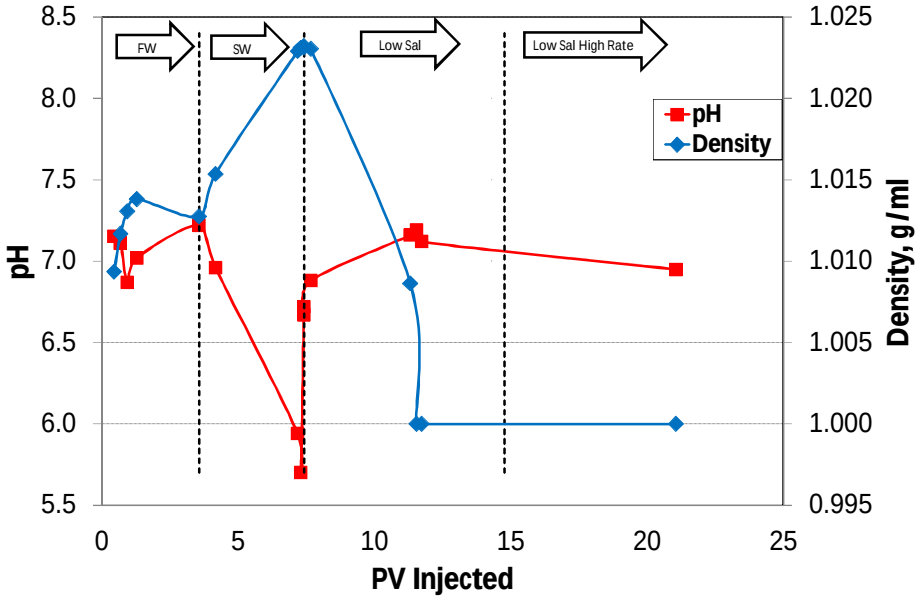

Figure 4.8. pH and Density as the function of PV injected on Oil recovery test of core #60. The core was flooded with FW, SW and LS fluid at a rate of 4 PV/D. The oil recovery is plotted against PV injected. At the end the flooding rate was increased to 16 PV/D.

During the FW flooding the density stabilized at ρ= 1.013 g/ml. During SW flooding the density was increased to ρ =1.023 g/ml. When switching to LS, the density was decreased to ρ=1.000 g/ml.

The pH initially was at pH 6.8 and increased to pH 7.2 during FW flooding. When switching to SW, the pH decreased down to 5.7. A sharp increase in pH was observed when the LS brine was introduced with a pH of 6.8, which increased to pH 7.2 before it gradually decreased again.

CAHPATER V
DISCUSSION

5.1. Introduction

The new chemical mechanisms by Tor Austad et al,(2010) proposed that the following parameters will play a major role:

- Clay properties/types and the amount present in the rock.
- Polar components in the crude oil, both acidic and basic.
- The formation brine composition and the initial pH is important to enhance absorption of polar components.
- A gradient in the calcium concentration between FW/SW/and LS brine is important when the smart water (LS) is introduced, Ca^{2+} ions will be desorbed from the clay surface.
- H^+ will compensate the unbalanced negative charge on the clay surface, and a local pH increase will occur close to the clay surface. These phenomenon of chemical reaction can be illustrated by the equation 2.16 (Clay -Ca^{2+} + H_2O ↔ Clay -H^+ + Ca^{2+} + OH-).
- The local increase in pH close to the clay surface causes reactions between the adsorbed protonated basic and acidic material as in an ordinary acid-base proton transfer reaction, as shown in the equation 2.17 (Clay-NHR_3^+ + OH^-↔ Clay + R_3N + H_2O) and 2.18(Clay – ROOH + OH^-↔ Clay + $RCOO^-$ + H_2O).
- Increased pH will promote desorption of polar components from the clay surface, and the wetness of the clay surface.
- Adsorption/ desorption of polar components are influenced by;
  - Effect of pH.
    - ✓ Absorption decreases with increasing pH.
  - Effect of salinity/ Calcium concentration.
    - ✓ More absorption with LS compares to HS brine.

- ✓ More water wetness at higher pH.

- Temperature effect
  - ✓ Lower adsorption at higher temperature (more water-wet)
  - ✓ High temperature and high salinity.
    - o Reduced adsorption
- Anhydrate dissolution at LS.
  - ✓ Increases Ca^{2+} concentration due to anhydrate dissolution.

5.2. pH Screening

The reservoir core#48 and core#60 were both cleaned with Toluene and methanol prior to use. The cores were100% saturated with formation water. During the pH screening experiments, effluent samples were analysed for measuring the pH and salinity and chemical analysis for ions concentration of Ca^{2+}, Mg^{2+} and SO_4^-.

5.2.1. Initial pH on FW flooding.

The brines were used in the experiment have the salinity and Ca^{2+} ion composition as follows:

- FW; salinity of 2200 ppm and Ca^{2+} concentration of 3.5 mM.
- SW; salinity of 33000 ppm and Ca^{2+} concentration of 13 mM.
- LS; salinity of 1200 ppm and Ca^{2+} concentration of 0.3 mM.

The initial pH flooding with FW (pH screening on core#48 and core#60 was from pH is 5 – 6). Taken into consideration that the stabilized crude oil a Base Number of 1.35 mg KOH/g, and those should be enough basic material present in the crude oil to absorb onto the clay surface. Previous low salinity flooding experiment indicating that there appeared to be no restriction to the type of polar components present in crude provided that a significant amount is present (Tor Austad et al., 2010).

On core#48 the pH stabilized at 6 during FW flooding while on core #60, pH was increased gradually to 7.5.

5.3. pH changes during SW flooding

When introducing SW, a small decline in pH was observed on core#48. Those are still favourable for polar component to absorb onto the clay surface. On core #60 the pH decreased almost 1pH unit and stabilized at 6.5.

5.4. pH changes during LS flooding

Based on the clay content presented in table 3.3 and related to the brine composition and ion concentration listed in table 3.2, it should be expected a pH increase when introducing LS flooding on core#48 and cor#60. The Results of the pH screening on both cores showing an increase of about 1 pH unit (presented in fig 4.1 and fig 4.3) when introducing LS flooding.

The pH increased is large enough to promote desorption of polar components from the clay surface. This desorption process, will induce positive capillary pressure, and consequently spontaneous imbibition could occur. Evidently an increase of local pH close to the clay surface and an oil recovery could be observed as shown in figure 4.5.

5.5. Ion Concentrations

From the chemical analysis on core#48 (fig 4.4) and core#60 (fig 4.2), we observed a very low dissolution of Anhydrate. This could give an increased in Ca^{2+} concentration in the LS brine and reduces the smart water effect.

5.6. Oil recovery

Core#15 mildly cleaned and saturated (Swi = 20%), and aged with crude oil. The core was successively flooded with FW-SW-LS.

Based on the pH screening tests performed on core#48 and core#60, an initial pH that could promote adsorption of polar components is expected also for core#15 (fig 4.5 and fig 4.6). The oil recovery with FW was 42% OOIP. The pH of the first produced brine was 6.6.

No improved oil recovery were observed when switching to SW, but a decrease in pH to 6.3 was observed in the produced brine. A rapid pH increase was observed when switching from SW to LS followed by an increased oil recovery of 2.3% after 0.4 PV injected.

The result with increased pH and enhanced oil recovery are in line with the proposed chemical LS mechanism.

For the second core, core#60, no increased LS EOR effects were observed in the oil recovery test. This could be explained by prior to using for oil recovery test, the core had been used in pH screening, changing the initial pH condition of the core. The initial pH in the pH screening test gradually increased from pH 5 to pH 7.5 during FW flooding.

CHATPER VI
CONCLUSION

Conclusion

Based on the observations and discussions on the experimental results from three preserved cores from a high temperature reservoir (130^{0}C), it can be concluded that;

- Both Core#48 and core#60 showed an initial pH in the range of 5 – 6 which is favourable for polar components to absorb onto the clay surface to promote less water-wet initial wetting conditions.
- During SW flooding both cores showed a decrease in pH which indicates no absorption of polar components from the clay surface.
- During LS water flooding, an increase of one pH unit was observed from both cores, and consequently polar components could be desorbed form the clay surface.
- When introducing LS flooding oil recovery test on core#15, an increase oil recovery was observed. This could be explained by a low initial pH and a pH increase when the LS brine was introduced. This observation is in line with the proposed chemical LS mechanism.
- It is important to avoid that cores used in oil recovery tests, previously have been flooded with other brines.
- For core#60, the initial pH was about 5. However at the end of the pH screening test, the pH ended up at pH 7.3. During the core restoration, the initial wetting of the core became too water-wet and consequently no increase in oil recovery was observed when introducing LS brine.

REFERENCES

1. Willhite, G. Paul., 1998. ***Enhanced Oil Recovery***. Henry L. Doherty Memorial Fund of AIME Society of Petroleum Engineers Richardson, TX USA.
2. Tao Gang, PetroTel Inc., and Mohan Kelkar., U. of Tulsa.,2007. ***A More General Capillary Pressure Curve and Its Estimation From Production Data.*** SPE-108180-MS presented at the conference paper Rocky Mountain Oil & Symposium, Denver, Colorado, USA, 16 – 18 April.
3. T. Chen, O. Chen, P. Chen., 2001. ***Capillary Pressure During Immiscible Displacemen.*** PETSOC-01-02-02 Journalpaper, Petroleum Technology of Canada.
4. Anderson, W.G.,Inc, Conoco.,1987. ***Wettability Literature Survey- Part 4 Effects of Wettability on Capillary Pressure.*** SPE- 15271-PA Journal Paper.The Society Of Petroleum Engineers.
5. Austad, T.,RezaeiDoust,Alireza., and Puntervold, Tina.,2010. ***Chemical Mechanism of Low Salinity Water Flooding in Sandstone Reservoirs.*** SPE 12967 – MS presented at the 2010 SPE Improved Oil Recovery Symposium held in Tulsa, USA, 24 – 28 April.
6. AdeelZahid, Alexander Shapiro., 2012. ***Experimental Studies of Low Salinity Water Flooding Carbonate: A New Promising Approach.*** Center for Energy Resources Engineering, Department of Chemical and Biochemical Engineering Technical University of Denmark.
7. Cliff Black, Black ., 1991. ***The BP Relative Permeability Handbook***. Head, Waterflood Group, Reservoir Management Branch, Exploration & Production Division, B P Research, Sunbury.
8. Ursin, J.-R., Zolotukin, A. B., 2000. ***Introduction to Petroleum Reservoir Engineering.*** Hoyskoleforlaget AS.
9. Doust, A. R., 2011. ***Low Salinity Water Flooding in Sandstone Reservoirs.*** Doctor of Philosophy Theses. Department of Petroleum Engineering, University of Stavanger, Norway.
10. Melberg, Elin., 2010. ***Experimental Study of Low Salinity EOR Effects from the Varg Field.*** Master's Thesis, Department of Petroleum Engineering, University of Stavanger, Norway.
11. Dubey, S.T., P.H. Doe., 1993. ***Base Number and Wetting Properties of Crude Oils***. SPE-22598-PA, Shell Development Co.
12. Fink, J. Karl., 2003. ***Oil Field Chemical***. Elsevier Science, USA.

13. Bernard, George G,. 1967. ***Effect of Floodwater Salinity on Reservoir of Oil from Cores Containing Clays***. SPE 1725-MS presented at the SPE Conference, Los Angeles, California, USA 26 – 27 October.

14. Nasralla, Ramez A,. B. Alotaibi, Mohammed,. Nasr-Eldin, Hisham A., 2011***. Efficiency of Low Salinity Flooding in Sandstones Reservoir.*** SPE 144602-MS presented at the SPE conference held in Anchorage, Alaska, USA, 7 – 11 May.

15. Jerauld R. Gary,. Lin, C.Y., Webb J. Kevin,. 2008. ***Modeling Low Salinity Waterflooding.*** SPE 102239-PA presented at 2006 Annual Technical Conference and Exhibition, San Antonio, Texas, USA, 24-27 September.

16. Nasralla, Ramez A,. B. Alotaibi, Mohammed,. Nasr-Eldin, Hisham A., 2011***. Investigation of Wettability Alteration by Low Salinity Water in Sandstone Rock.*** SPE 146322 presented at the SPE conference on Offshore Europe Oil and Gas Conference and Exhibition, Aberdeen, UK, 6 – 8 of September.

17. Strand, S,.Hamso, D,.Austad, Tor,.Aksulu, Hakan,, and Putervold, T,. 2012. ***Evaluation of Low salinity EOR-effects in Sandstones: Effects of Temperature and pH gradient***. 33rd IEA EOR Symposium. Canada, 26 – 30 August.

18. Skauge, A., Standal, S., . Boe , S.O., Skauge, T,. Blokhus, A.M., 1999. ***Effects of Organic Acids and Bases, and Oil Composition on Wettability***. SPE- 56673-MS, presented at annual conference and exhibition, Houston, Texas, USA, 3 – 6 October.

19. Buckley, J.S., Takamura, K., and Morrow, N.R.,. 1989. ***Influence of Electrical Surface Charges on the Wetting Properties of Crude Oils.*** SPE- 16964-PA, Journal SPE Reservoir Engineering, New Mexico Petroleum Recovery Research Center, New Mexico Inst. of Mining and Technology.

20. Buckley, J.S., Liu,Y., Monsterleet, S,.1998. ***Mechanisms of Wetting Alteration by Crude Oils.*** SPE- 37230-PA Journal Paper. New Mexico Petroleum Recovery Research Center, New Mexico Inst. of Mining and Technology.

21. Austad, T., RezaeiDoust, Alireza., and Puntervold, Tina.,2010. ***A Discussion of the Low-Salinity EOR Potential for a North Sea Sandstone Field***. SPE 134459 – MS presented at the SPE Annual Technical Conference and Exhibition, Florence, Itali. 19-22 September.

22. Morrow, Norman, R., 1990. ***Wettability and Its Effect on Oil Recovery.*** SPE-12621-PA Journal Paper, New Mexico Petroleum Recovery Research Center, New Mexico Inst. of Mining and Technology.

23. Buckley, J.S., Liu,Y., Monsterleet, S,.1997. ***Evolution of Wetting Alteration by Adsorption From Crude Oil.*** SPE-28970-PA Journal Paper, New Mexico Petroleum Recovery Research Center, New Mexico Inst. of Mining and Technology.

24. Morrow, Norman, R., Yin, P., Xie, X., Pu, H.,2010. ***Low Salinity Waterflooding and Mineral Dissolution.*** SPE-134042-MS presented at the SPE Annual Technical Conference and Exhibition, Florence, Italy. 19-22 September.
25. Berg, R. Robert., 1986. ***Reservoir Sandstone.*** Prentice-Hall, Inc., Englewood Cliffs, New Jersey, USA.
26. Nasralla, Ramez A., Bataweel, Mohammed A., Nasr-El-Din, Hisham A., 2011. ***Investigation of Wettability Alteration by Low Salinity Water.*** SPE-146322-MS presented at Offshore Europe, Aberden, UK, 6 – 8 September.
27. Donaldson Erle C., Chilinggarian, George, V., Yen, T. Fu., 1989. ***Enhanced Oil Recovery, II Process and Operations.*** Elsevier Science Publishers B.V. Amsterdam, The Netherlands.
28. Mazzullo, L., J., Mazzullo, M., J., 1987. ***Geology and Clay Mineralogy of the Morrow Formation.*** SPE-13849-PA Journal Paper, The Society of Petroleum Engineering, Southeastern New Mexico.
29. Hughes, Richard V., 1950. ***The Application of Modern Clay Concepts to Oilfield Development.*** Conference paper, American Petroleum Institute.
30. Anderson, William G., Inc, Conoco., 1986. ***Wettability Literature Survey- Part 1: Rock/Oil/Brine Interactions and the Effects of Core Handling on Wettability.*** SPE-13932-PA Journal Paper. The Society of Petroleum Engineers.
31. Anderson, William G., Inc, Conoco., 1986. ***Wettability Literature Survey- Part 5: Rock/Oil/Brine Interactions and the Effects of Core Handling on Wettability.*** SPE-13932-PA Journal Paper. The Society of Petroleum Engineers.
32. Ahmed, Tarek.,2000. ***Reservoir Engineering Handbook second edition.*** Gulf Publishing Company, Huston, USA.
33. Daniel,Longeron., WibekeHammervold, L., Svein, M. Skjaeveland., 1995. ***Water-Oil Capillary Pressure and Wettability Measurements Using Micropore Membrane Technique.*** SPE-30006-MS presented at the International Meeting on Petroleum Engineering, Beijing, China 14 – 17 November.
34. Hadley,G.F.,Handy.A, L.L., 1956.***Theoretical and Experimental Study of the Steady State Capillary End Effect.*** SPE-00707-G, presented at the Fall Meeting of the Petroleum Branch of AIME, Los Angeles ,California, USA. 14 – 17 October.
35. Blyth, F. G. H., De Freitas, M. H., 2005. ***A Geology for Engineers, Seventh Edition.*** Elsevier Butterworth-Heinemann, UK.
36. Simon, D.E., Anderson, M.S., Halibuton Service., 1990. ***Stability of Clay Minerals in Acid.*** SPE-19422-MS, presented at SPE Formation Damage Control Symposium, Lafayette, Louisiana, USA, 22 -23 February.

37. Fink, K. Johanes.,2003. ***Oil Field Chemicals.*** Elsevier Science, Boston, USA.

APPENDIX

A1. History of Low Salinity

A brief summary of the main history of Low Salinity (Zhang, 2007)

1942) The question of Low Salinity injection was raised. Initial studies with Kansas crude oil and cores showed no significant difference in recoveries of brines versus water. Documented results for oil recovery of Bradford crude oil and sandstones with a range of permeability showed overall recoveries to be less for fresh water than for a brine of 40% higher viscosity. The difference was explained using swelling of clays (Smith, 1942).

1959) Observation of increased oil recovery of heavy oil through injection of fresh water. The effect of clay swelling and emulsification were suggested as possible causes (Martin, 1959).

1967) From laboratory test on recovery on mineral oil concluded that swelling clays and/dispersion accompanied by increased pressure drop, resulted in additional oil production by injection of fresh water or 1000 ppm NaCl (Bernard, 1967).

1999) Migration of Fines (Tang and Morrow, 1999)

2005) pH increase (McGuire et al., 2005).

2006) Multi Ionic Exchange (Larger et al., 2006).

2008) Salting in effect (Austad et al.,2008. This was only working proporsal).

2009) Double layer effect (Lightelm et al., 2008).

2010) Desorption by pH increase (Austad et al., 2010)

A2. Crude oil properties

Table A.1. Crude oil properties

	AN (20^0C) [mg KOH/g]	BN (20^0C) [mg KOH/g]	Asphaltene [g/100ml]	Density g/cm^3@ 20^0C	Viscosity [cp] @ 20^0C
Crude Oil	0.0	1.35	0.57	0.847	Not Measured

A3. Brine properties

Table A.2. Brine properties

SALT	FW		SW		LS	
	m[g/l]	mMole/liter [molar]	m[g/l]	mMole/liter [molar]	m[g/l]	mMole/liter [molar]
SSW	22.11		38.67		1.94	
NaCl	21.52	0.368	23.38	0.400	0.90	0.015
Na2SO4	0.00	0.000	3.41	0.024	0.12	0.001
KSCN	0.00	0.000		0.000	0.00	0.000
NaHCO3	0.23	0.003	0.17	0.002	0.00	0.000
KCl	0.23	0.003	0.00	0.00	0.03	0.000
AlC3	0.00	0.000				
MgCl2 x 6H20	0.28	0.001	9.05	0.045	0.36	0.002
CaCl2 x 2H2O	0.51	0.003	1.91	0.013	0.05	0.000
BaCl2 x 2H2O	0.15	0.001	0.00	0.00	0.00	0.000
SrCl2 x 2H2O	0.23	0.001	0.00	0.00	0.00	0.000
IONS	**m[g/l]**	**mMole/liter [molar]**	**m[g/l]**	**mMole/liter [molar]**	**m[g/l]**	**mMole/liter [molar]**
HCO_3^-	165.6	2.7	123.5	2.0	0.0	0.0
Cl^-	13625.5	384.0	18617.4	525.1	705.5	19.9
SO_4^{2-}	0.0	0.00	2306.0	24.0	78.4	0.8
SCN^-	0.0	0.0	0.0	0.0	0.0	0.0
Mg^{2+}	34.0	1.4	1082.4	44.5	42.9	1.8
Ca^{2+}	140.1	3.5	520.0	13.0	12.6	0.3
Na^+	8527.6	370.9	10347.4	450.1	390.8	17.0
K^+	120.1	3.1	393.5	10.1	14.7	0.4
Ba^{2+}	84.1	0.6	0.0	0.0	0.0	0.0
Sr^{2+}	76.0	0.9	0.0	0.0	0.0	0.0
Al^{3+}	0.0	0.0	0.0	.0	0.0	0.0
TDS, g/l		222.19	33390.0	33.43	1245.0	

A4. Reservoir Clay Content

Table A.3. Reservoir Clay content

Core#	Kaolinite	Illite
Core#15	6 – 8%	2 – 4%
Core#48		
Core#60		

A5. Procedure of AN and BN measurement

The AN and the BN of the crude oil are measured by the automatic titrator, MettlerToled DL55, shown in figure A.1. There are different type of solvents are used as shown in table A.4.

- Calibrate the pH probes with standard buffer solution with pH 4.00, pH 7.00 and pH 10.00.
- Standardize the titrtant with 50 ml standard solution.
- Make a sample of 1 ml spiking solution and 50 ml titration solvent. The spikngsilutionia added to improve the accuracy of the measurements of oil that have low AN. The total acid/base content of the sample is measured using the titrant.
- Make a new sample of 1 ml spiking solution and 50 ml titration solvent (blank), and add 1 ml oil to it. The total acid/base content of new sample is also measured using titrant.
- The difference in the total acid/base content between the bank and the sample containing oil is related to the amount of oil added.

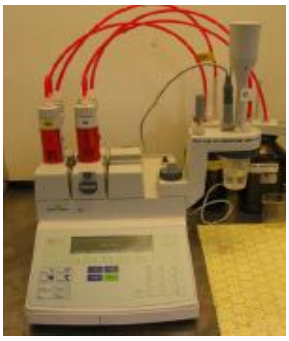

Figure A.1. measurement of AN and BN using Titrator equipment

Table A.4. Material for AN and BN measurement

	AN	BN
Titrant	0.05 M tetra butyl ammonium hydroxide in ethanol or methanol	5 ml 70% $HCLO_4$, 15 ml $(CH_3CO)_2O$ diluted to 1000 ml glacial HAc
Skiping solution	~0.5 g stearic acid diluted to 100 ml with acid titration solvent or decane	~0.5 g quinoline diluted to 100 ml with n-decane
Standard solution	~0.2 g potassium hydrogen phthalate (KHP) diluted to 599 ml with dionized water	~0.2 g KHP diluted to 250 ml with glacial acetic acid (HAc)
Titration solvent	6 ml dionized water and 494 ml HPLC grade 2-propanol and 500 ml HPLC grade toluene	Methyl isobutyl ketone (MIBK)

A6. Ions Concentration

Table A.6.1. Sulfate Core#48

Data Chemical Analysis Core#48

SULFATE

Reference				Sample	
Type	Dilution Ratio	Area (µS*min)	SO_4^{2-} amount (mole/liter)	Dilution Ratio	Base Area
				200	
Pelican SW	200	1.25850	0.024	50	

Sample No.	Sample Area	Pore Volume	SO_4^{2-} amount (mole/liter)	SO_4^{2-} amount (mmole/liter)	SO_4^{2-} amount (g/liter)
1 1:200	0.02590	0.000	0.00049	0.49392	0.04745
5	0.01270	0.868	0.00024	0.24219	0.02327
9	0.00870	1.737	0.00017	0.16591	0.01594
31	0.00330	6.516	0.00006	0.06293	0.00605
43	0.00320	9.122	0.00006	0.06103	0.00586
53	0.02300	11.294	0.00044	0.43862	0.04213
55	0.01860	11.728	0.00035	0.35471	0.03407
57	0.01850	12.163	0.00035	0.35280	0.03389
59	0.44290	12.597	0.00845	8.44625	0.81135
61	1.05660	13.032	0.02015	20.14970	1.93558
69	1.26580	14.769	0.02414	24.13921	2.31881
77	1.27480	16.507	0.02431	24.31085	2.33530
85	1.27660	18.245	0.02435	24.34517	2.33860
2-7	1.26110	20.417	0.02405	24.04958	2.31020
2-9	1.23370	20.851	0.02353	23.52706	2.26001
2-11 1:200	0.73220	21.285	0.01396	13.96329	1.34131
2-13 1:50	1.35060	21.720	0.00644	6.43909	0.61854
2-15	0.64740	22.154	0.00309	3.08653	0.29649
2-25	0.17030	24.326	0.00081	0.81192	0.07799
2-35	0.14280	26.498	0.00068	0.68081	0.06540
2-45	0.13470	28.670	0.00064	0.64219	0.06169
2-55	0.13170	30.842	0.00063	0.62789	0.06032
2-61	0.13410	32.146	0.00064	0.63933	0.06141
2-63 1:50	0.12910	32.580	0.00062	0.61549	0.05912
2-65 1:200	0.00930	33.014	0.00018	0.17735	0.01704
2-67	0.02220	33.449	0.00042	0.42336	0.04067
2-69	0.02680	33.883	0.00051	0.51108	0.04909
2-73	0.01970	34.752	0.00038	0.37569	0.03609
2-79	0.01490	36.055	0.00028	0.28415	0.02730
2-83	0.01160	36.924	0.00022	0.22122	0.02125
2-87 1:200	0.01050	37.793	0.00020	0.20024	0.01923

Table A.6.2. Calcium Core#48

Data Chemical Analysis Core#48

CALCIUM

Reference				Sample	
Type	Dilution Ratio	Area (µS*min)	Ca^{2+} amount (mole/liter)	Dilution Ratio	Base Area
				200	
Pelican SW	200	0.32080	0.013	50	

Sample No.	Sample Area	Pore Volume	Ca^{2+} amount (mole/liter)	Ca^{2+} amount (mmole/liter)	Ca^{2+} amount (g/liter)
1 1:200	0.08660	0.000	0.00351	3.50935	0.14065
5	0.07830	0.868	0.00317	3.17300	0.12717
9	0.07580	1.737	0.00307	3.07170	0.12311
31	0.07820	6.516	0.00317	3.16895	0.12701
43	0.08150	9.122	0.00330	3.30268	0.13236
53	0.08390	11.294	0.00340	3.39994	0.13626
55	0.08050	11.728	0.00326	3.26216	0.13074
57	0.09790	12.163	0.00397	3.96727	0.15900
59	0.16090	12.597	0.00652	6.52026	0.26132
61	0.31200	13.032	0.01264	12.64339	0.50672
69	0.29780	14.769	0.01207	12.06796	0.48366
77	0.28280	16.507	0.01146	11.46010	0.45930
85	0.28510	18.245	0.01155	11.55330	0.46303
2-7	0.28590	20.417	0.01159	11.58572	0.46433
2-9	0.26660	20.851	0.01080	10.80362	0.43299
2-11 1:200	0.09430	21.285	0.00382	3.82138	0.15315
2-13 1:50	0.05180	21.720	0.00052	0.52478	0.02103
2-15	0.03010	22.154	0.00030	0.30494	0.01222
2-25	0.01710	24.326	0.00017	0.17324	0.00694
2-35	0.02610	26.498	0.00026	0.26442	0.01060
2-45	0.01270	28.670	0.00013	0.12866	0.00516
2-55	0.02080	30.842	0.00021	0.21072	0.00845
2-61	0.02070	32.146	0.00021	0.20971	0.00840
2-63 1:50	0.03790	32.580	0.00038	0.38396	0.01539
2-65 1:200	0.07940	33.014	0.00322	3.21758	0.12895
2-67	0.24020	33.449	0.00973	9.73379	0.39011
2-69	0.20130	33.883	0.00816	8.15742	0.32693
2-73	0.12140	34.752	0.00492	4.91958	0.19717
2-79	0.09050	36.055	0.00367	3.66739	0.14698
2-83	0.08290	36.924	0.00336	3.35941	0.13464
2-87 1:200	0.08430	37.793	0.00342	3.41615	0.13691

Table A.6.3. Magnesium Core#48

Data Chemical Analysis Core#48

MAGNESIUM

Reference				Sample	
Type	Dilution Ratio	Area (µS*min)	Mg^{2+} amount (mole/liter)	Dilution Ratio	Base Area
				200	
Pelican SW	200	1.01316	0.0445	50	

Sample No.	Sample Area	Pore Volume	Mg^{2+} amount (mole/liter)	Mg^{2+} amount (mmole/liter)	Mg^{2+} amount (g/liter)
1 1:200	0.01390	0.000	0.000611	0.61051561	0.01483858
5	0.01110	0.868	0.000488	0.48753405	0.01184952
9	0.01280	1.737	0.000562	0.56220143	0.01366431
31	0.01180	6.516	0.000518	0.51827944	0.01259678
43	0.01170	9.122	0.000514	0.51388724	0.01249003
53	0.03470	11.294	0.001524	1.52409294	0.03704308
55	0.03030	11.728	0.001331	1.33083620	0.03234597
57	0.03210	12.163	0.001410	1.40989577	0.03426752
59	0.05410	12.597	0.002376	2.37617948	0.05775304
61	0.32840	13.032	0.014424	14.42398042	0.35057484
69	0.97190	14.769	0.042688	42.68777883	1.03752646
77	1.00140	16.507	0.043983	43.98347744	1.06901842
85	1.01480	18.245	0.044572	44.57203206	1.08332324
2-7	0.99320	20.417	0.043623	43.62331715	1.06026472
2-9	0.94050	20.851	0.041309	41.30862845	1.00400621
2-11 1:200	0.29450	21.285	0.012935	12.93502507	0.31438578
2-13 1:50	0.11320	21.720	0.001243	1.24299222	0.03021093
2-15	0.02200	22.154	0.000242	0.24157093	0.00587138
2-25	0.01300	24.326	0.000143	0.14274646	0.00346945
2-35	0.01200	26.498	0.000132	0.13176596	0.00320257
2-45	0.00990	28.670	0.000109	0.10870692	0.00264212
2-55	0.00930	30.842	0.000102	0.10211862	0.00248199
2-61	0.01280	32.146	0.000141	0.14055036	0.00341608
2-63 1:50	0.02180	32.580	0.000239	0.23937483	0.00581801
2-65 1:200	0.26690	33.014	0.011723	11.72277824	0.28492213
2-67	0.91170	33.449	0.040044	40.04367523	0.97326153
2-69	0.69240	33.883	0.030412	30.41158356	0.73915354
2-73	0.31140	34.752	0.013677	13.67730664	0.33242694
2-79	0.13190	36.055	0.005793	5.79331004	0.14080640
2-83	0.08480	36.924	0.003725	3.72458447	0.09052603
2-87 1:200	0.06340	37.793	0.002785	2.78465395	0.06768101

Table A.6.4. Sulfate Core#60

Data Chemical Analysis Core#60					
SO_4^{2-}					
Reference				Sample	
Type	Dilution Ratio	Area (µS*min)	SO_4^{2-} amount	Dilution Ratio	Base Area
Pelican				200	
SW	200	1.22822	0.024	50	
					96.06

Sample No.	Pore Volume	Area (µS*min)	SO_4^{2-} amount	SO_4^{2-} amount (mmole/liter)	SO_4^{2-} amount (g/liter)
1	0.000000		0	0	0
1-3 1:200	0.342358	0.1229	0.00240152	2.401519812	0.230689993
1-7	1.027759	0.066	0.001289669	1.289668898	0.123885594
1-19	3.083962	0.0091	0.000177818	0.177817984	0.017081196
1-31	5.140164	0.0042	8.20698E-05	0.082069839	0.007883629
1-77	13.02228	0.0028	5.47132E-05	0.054713226	0.005255752
2-33	20.56169	0.0029	5.66673E-05	0.05666727	0.005443458
2-81	28.7865	0.0029	5.66673E-05	0.05666727	0.005443458
3-29	34.95511	0.0041	8.01158E-05	0.080115795	0.007695923
3-33	35.64051	0.0029	5.66673E-05	0.05666727	0.005443458
3-35	35.98321	0.003	5.86213E-05	0.058621314	0.005631163
3-37	36.32591	0.0028	5.47132E-05	0.054713226	0.005255752
3-39	36.66861	0.0938	0.001832893	1.83289307	0.176067708
3-41	37.01131	0.5726	0.011188855	11.18885471	1.074801384
3-45	37.69671	1.1419	0.022313226	22.31322598	2.143408488
3-49	38.38211	1.2066	0.023577492	23.57749231	2.264853911
3-61	40.43831	1.1638	0.022741162	22.74116157	2.18451598
3-87	44.89342	1.2351	0.024134395	24.13439479	2.318349963
4-27	49.69123	1.2117	0.023677149	23.67714854	2.274426889
4-35	51.06203	1.1601	0.022668862	22.66886195	2.177570879
4-41	52.09013	1.0082	0.019700669	19.70066944	1.892446306
4-43	52.43283	1.0999	0.021492528	21.49252759	2.0645722
4-45 1:50	52.77553	3.1981	0.015623069	15.62306857	1.500751967
4-47	53.11823	1.4687	0.00717476	7.174760268	0.689207471
4-49	53.46093	0.692	0.003380496	3.380495748	0.324730422
4-51	53.80363	0.4813	0.002351203	2.351203184	0.225856578
4-55	54.48903	0.2783	0.001359526	1.359525963	0.130596064
4-87	59.97224	0.1287	0.000628714	0.628713588	0.060394227
5-19	63.39925	0.1212	0.000592075	0.592075267	0.05687475
5-21 1:50	63.74195	0.0593	0.000289687	0.289686991	0.027827332
5-23 1:200	64.08465	0.0184	0.000359544	0.359544056	0.034537802
5-25	64.42735	0.0182	0.000355636	0.355635969	0.034162391
5-27	64.77005	0.0504	0.000984838	0.984838068	0.094603545
5-29	65.11275	0.0164	0.000320463	0.320463181	0.030783693
5-33	65.79815	0.0118	0.000230577	0.230577167	0.022149243
5-35	66.14085	0.0106	0.000207129	0.207128641	0.019896777
5-37	66.48355	0.009	0.000175864	0.175863941	0.01689349
5-39	66.82625	0.0085	0.000166094	0.166093722	0.015954963
5-41	67.16895	0.0073	0.000142645	0.142645196	0.013702498
5-45	67.85435	0.0057	0.00011138	0.111380496	0.01069921
5-49	68.53975	0.0047	9.18401E-05	0.091840058	0.008822156
5-59	70.25326	0.0043	8.40239E-05	0.084023883	0.008071334
5-71	72.30946	0.0039	7.62077E-05	0.076207708	0.007320512
5-83	74.36566	0.003	5.86213E-05	0.058621314	0.005631163
6-9	76.76456	0.0029	5.66673E-05	0.05666727	0.005443458

Table A.6.5. Magnesium Core#60

Data Chemical Analysis Core#60					
Mg^{2+}					
Reference				Sample	
Type	Dilution Ratio	Area (µS*min)	Mg^{2+} amount (mmole/liter)	Dilution Ratio	Base Area
Pelican				200	
SW	200	0.919156	0.0445	50	
					24.305

Sample No.	Pore Volume	Area (µS*min)	Mg^{2+} amount (mmole/liter)	Mg^{2+} amount (mmole/liter)	Mg^{2+} amount (g/liter)
1	0.000000		0	0	0
1-3 1:200	0.342358	0.0279	0.001350751	1.350750689	0.032829995
1-7	1.027759	0.0278	0.001345909	1.345909289	0.032712325
1-19	3.083962	0.0194	0.000939232	0.939231662	0.022828026
1-31	5.140164	0.0214	0.00103606	1.036059668	0.02518143
1-77	13.02228	0.019	0.000919866	0.919866061	0.022357345
2-33	20.56169	0.0218	0.001055425	1.05542527	0.025652111
2-81	28.7865	0.0251	0.001215191	1.21519148	0.029535229
3-29	34.95511	0.0258	0.001249081	1.249081282	0.030358921
3-33	35.64051	0.0263	0.001273288	1.273288284	0.030947272
3-35	35.98321	0.0261	0.001263605	1.263605483	0.030711931
3-37	36.32591	0.0284	0.001374958	1.374957691	0.033418347
3-39	36.66861	0.0435	0.002106009	2.106009139	0.051186552
3-41	37.01131	0.1681	0.008138394	8.138393936	0.197803665
3-45	37.69671	0.6448	0.031217349	31.21734926	0.758737674
3-49	38.38211	0.7639	0.036983457	36.98345704	0.898882923
3-61	40.43831	0.9725	0.047082618	47.0826181	1.144343033
3-87	44.89342	1.0133	0.049057909	49.05790943	1.192352489
4-27	49.69123	1.0041	0.048612501	48.6125006	1.181526827
4-35	51.06203	0.9623	0.046588795	46.58879527	1.132340669
4-41	52.09013	0.8432	0.040822687	40.82268749	0.992195419
4-43	52.43283	0.8579	0.041534373	41.53437334	1.009492944
4-45 1:50	52.77553	1.6422	0.019876369	19.87636901	0.483095149
4-47	53.11823	0.3639	0.004404464	4.40446394	0.107050496
4-49	53.46093	0.0796	0.000963439	0.963438664	0.023416377
4-51	53.80363	0.033	0.000399416	0.399415526	0.009707794
4-55	54.48903	0.0162	0.000196077	0.196076713	0.004765645
4-87	59.97224	0.0129	0.000156135	0.15613516	0.003794865
5-19	63.39925	0.0172	0.00020818	0.208180214	0.00505982
5-21 1:50	63.74195	1.0862	0.013146823	13.14682257	0.319533522
5-23 1:200	64.08465	0.7783	0.037680619	37.68061868	0.915827437
5-25	64.42735	0.7593	0.036760753	36.76075262	0.893470093
5-27	64.77005	0.6272	0.030365263	30.3652628	0.738027712
5-29	65.11275	0.4606	0.02229949	22.29948987	0.541989101
5-33	65.79815	0.0616	0.002982303	2.982302597	0.072484865
5-35	66.14085	0.1943	0.009406841	9.40684082	0.228633266
5-37	66.48355	0.155	0.00750417	7.504170495	0.182388864
5-39	66.82625	0.1277	0.006182468	6.182468208	0.15026489
5-41	67.16895	0.1054	0.005102836	5.102835936	0.124024427
5-45	67.85435	0.0724	0.003505174	3.505173831	0.08519325
5-49	68.53975	0.0581	0.002812854	2.812853585	0.068366406
5-59	70.25326	0.0361	0.001747746	1.747745515	0.042478955
5-71	72.30946	0.0277	0.001341068	1.341067888	0.032594655
5-83	74.36566	0.029	0.001404006	1.404006093	0.034124368
6-9	76.76456	0.0262	0.001268447	1.268446884	0.030829602

Table A.6.6. Calcium Core#60

Data Chemical Analysis Core#60					
Ca^{2+}					
Reference				Sample	
Type	Dilution Ratio	Area (µS*min)	Ca^{2+} amount (mole/liter)	Dilution Ratio	Base Area
Pelican				200	
SW	200	0.32534	0.013	50	

40.078

Sample No.	Pore Volume	Area (µS*min)	Ca^{2+} amount (mole/liter)	Ca^{2+} amount (mmole/liter)	Ca^{2+} amount (g/liter)
1	0.000000		0	0	0
1-3 1:200	0.342358	0.0778	0.003108772	3.108771660	0.124593351
1-7	1.027759	0.068	0.002717178	2.717178315	0.108899073
1-19	3.083962	0.0587	0.002345564	2.345564222	0.094005523
1-31	5.140164	0.086	0.003436431	3.436431398	0.137725298
1-77	13.02228	0.0983	0.003927921	3.927921005	0.157423218
2-33	20.56169	0.0987	0.003943904	3.943904407	0.158063801
2-81	28.7865	0.1054	0.004211626	4.211626388	0.168793562
3-29	34.95511	0.1102	0.004403427	4.403427210	0.176480556
3-33	35.64051	0.1092	0.004363469	4.363468706	0.174879099
3-35	35.98321	0.1034	0.004131709	4.131709379	0.165590648
3-37	36.32591	0.108	0.004315519	4.315518500	0.17295735
3-39	36.66861	0.1411	0.005638145	5.638145003	0.225965575
3-41	37.01131	0.2221	0.008874784	8.874783878	0.355683588
3-45	37.69671	0.3338	0.013338149	13.338148845	0.534566329
3-49	38.38211	0.3479	0.013901564	13.901563761	0.557146872
3-61	40.43831	0.3097	0.012375149	12.375148884	0.495971217
3-87	44.89342	0.3107	0.012415107	12.415107388	0.497572674
4-27	49.69123	0.2994	0.011963576	11.963576286	0.47947621
4-35	51.06203	0.2961	0.011831713	11.831713221	0.474191402
4-41	52.09013	0.2633	0.010521074	10.521074269	0.421663615
4-43	52.43283	0.264	0.010549045	10.549045222	0.422784634
4-45 1:50	52.77553	0.4805	0.004800015	4.800015369	0.192375016
4-47	53.11823	0.1315	0.001313636	1.313635840	0.052647897
4-49	53.46093	0.0641	0.000640335	0.640335037	0.025663348
4-51	53.80363	0.0421	0.000420563	0.420563261	0.016855334
4-55	54.48903	0.0379	0.000378607	0.378606831	0.015173805
4-87	59.97224	0.0424	0.00042356	0.423560149	0.016975444
5-19	63.39925	0.0388	0.000387597	0.387597495	0.015534132
5-21 1:50	63.74195	0.2696	0.002693203	2.693203212	0.107938198
5-23 1:200	64.08465	0.2094	0.008367311	8.367310869	0.335345085
5-25	64.42735	0.2153	0.008603066	8.603066047	0.344793681
5-27	64.77005	0.219	0.008750913	8.750912514	0.350719072
5-29	65.11275	0.1645	0.006573174	6.573174012	0.263439668
5-33	65.79815	0.1116	0.004459369	4.459369117	0.178722595
5-35	66.14085	0.1045	0.004175664	4.175663734	0.167352251
5-37	66.48355	0.1006	0.004019826	4.019825566	0.161106569
5-39	66.82625	0.0979	0.003911938	3.911937603	0.156782635
5-41	67.16895	0.095	0.003796058	3.796057940	0.15213841
5-45	67.85435	0.0914	0.003652207	3.652207323	0.146373165
5-49	68.53975	0.0933	0.003728128	3.728128482	0.149415933
5-59	70.25326	0.0975	0.003895954	3.895954201	0.156142052
5-71	72.30946	0.1058	0.00422761	4.227609790	0.169434145
5-83	74.36566	0.105	0.004195643	4.195642986	0.16815298
6-9	76.76456	0.1069	0.004271564	4.271564145	0.171195748

NOMENCLATURE

AN: Acid Number

BN: Base Number

CEC: Cation Exchange Capacity

DI: Deionized Water

EOR: Enhanced Oil Recovery

FW: Formation Water

Low Sal: Low Salinity

LS: Low Salinity

MIE: Multicomponent Ion Exchange

PV: Pore Volume

SW: Sea Water

TDS: Total Dissolved Solid

XRD: X-ray Diffraction Analysis